Chemical Engineering Journal 429 (2022) 131968

Contents lists available at ScienceDirect

Chemical Engineering Journal

journal homepage: www.elsevier.com/locate/cej

CO_2 gradient domestication produces gene mutation centered on cellular light response for efficient growth of microalgae in 15% CO_2 from flue gas

Zhenyi Wang [a], Jun Cheng [a,*], Wenlu Song [b], Xinxin Du [b], Weijuan Yang [a]

[a] State Key Laboratory of Clean Energy Utilization, Zhejiang University, Hangzhou 310027, China
[b] Department of Life Science and Engineering, Jining University, Jining 273155, China

ARTICLE INFO

Keywords:
CO_2
Microalgal domestication
Photosynthesis
Multi-omics analysis
CCUS

ABSTRACT

In order to promote photosynthetic reactions and biomass yield of microalgae in 15% CO_2 from coal-fired flue gas, a self-adaptive microalgal growth system with gene mutation centered on the cellular light response was established through CO_2 gradient domestication. The microalgae *Nannochloropsis oceanica* CCMP1779 was gradually acclimated to 0.04%, 3%, 6%, 10% and 12% CO_2 to obtain strains with a predominant adaptation to CO_2. The domesticated strain showed a 22.7-fold and 3.98-fold increase compared to wild-type under 6 mL/min and 12 mL/min 15% CO_2, respectively. A comprehensive analysis of the genome, transcriptome, photosynthetic fluorescence and RT-qPCR results were conducted to explore the effects of CO_2 gradient acclimation on microalgal growth. The CO_2 gradient domestication produced multi-targeted genetic mutations and natural selection, leading to successful transcriptional changes and apparent photosynthesis properties. Therefore, a self-adaptive microalgal growth system for high CO_2 was built based on photosynthesis enhancement (controlled by magnesium chelatase (EC 6.6.1.1)) in the competition between photosynthesis and respiration. This system was supported by improved cation transport, DNA and RNA synthesis, photosynthetic electron transfer, carbon fixation and metabolism. CO_2 gradient acclimation demonstrates a cost-effective method for generating microalgae mutants for efficient CO_2 fixation from coal-fired flue gas.

1. Introduction

Carbon dioxide (CO_2) has gradually but substantially influenced the environment with increasing CO_2 emissions because of global industrial prosperity. However, the development of carbon capture and utilization technologies are changing the conception of CO_2 from that of industrial waste to a useful energy source. It is predicted that the annual consumption of reutilized CO_2 will increase from 50.1 Mtpa to 326.7 Mtpa from 2018 to 2028 [57]. Because of the increased CO_2 proportion from flue gas of thermal power plants, which reached approximately to 40% in 2019, the goal to reduce 90% of the global CO_2 emissions from coal-fired power plants by the year 2040 was established within the sustainable development scenario of the International Energy Agency [26,71]. Photosynthetic CO_2 sequestration by microalgae and the related biomass utilization play an important role in carbon capture, utilization and storage (CCUS) technologies due to the fast microalgal growth rate, rapid environmental adaptability and high carbon concentration in biomass [32]. Accordingly, this method has shown potential in industrial production as a completely closed cycle for energy storage and utilization [84], because CO_2 released by flue gas from lots of industriesa is sequestrated by microalgae and then the microalgal biomass is converted to bio-gas and returns to the industry as energy. However, the tolerance to high CO_2 concentrations is a limitation for microalgal cultivation with flue gas [83]. Growth inhibition usually happens in the presence of>10% CO_2 [35,66], but the CO_2 concentration is commonly between 10% and 99% in industrial flue gas.

Many methods have attempted to improve the tolerance of microalgae to high CO_2 concentrations [22]. In some cases, certain microalgal strains with high adaptability to CO_2 were obtained by carefully screening for microalgae with special characteristics. Isolation from special native environmental and algal species with random mutagenesis are possible ways to obtain strains that could grow well under>10% CO_2 [20,21,34,53]. However, the randomness and nonrepeatability of strain isolation severely restrict the extensive application of this method. This process requires a lot of manpower and time, even though it is uncertain whether the desired results will be obtained. Genetic engineering is also an effective approach to improve the photosynthetic apparatus and Calvin cycle [7,61]. A breakthrough in which the

* Corresponding author.
E-mail address: juncheng@zju.edu.cn (J. Cheng).

https://doi.org/10.1016/j.cej.2021.131968
Received 28 June 2021; Received in revised form 13 August 2021; Accepted 19 August 2021
Available online 25 August 2021

carbonic anhydrase in *Nannochloropsis* was knocked down resulted in an increased biomass dry weight of 40% under 5% CO_2, which provides insight into solving the problem of microalgal survival under high CO_2 concentration flue gas[47]. However, the sophisticated, lengthy and expensive experimental process restricts the extensive development of genetic engineering to modify various microalgal species suitable for industrial production.

A simple and feasible method known as adaptive laboratory evolution (ALE) has been widely shown to be effective for improving the adaptability and growth of many microalgal species under high CO_2 concentrations [32]. With the help of stress domestication, a large number of microorganisms in a culture could in parallel accumulate beneficial mutations in a variety of genes directly through multi-cycle cultivation [77]. In recent years, this method has been successfully used in a large number of experiments to obtain growth advantages in high carbon environment with different microalgal species, including *Chlorella* sp., *Spirulina* sp., *Haematococcus pluvialis* and even mixed microalgal communities [1,11,13,28,30]. Unfortunately, previous studies have paid too much attention to macro experiments; thus, the mechanism of CO_2 gradient domestication that improves the microalgal characteristics is still not clear. The acceptance and widespread adoption of this approach have been affected by outstanding questions, including 1) is domestication simply a transient environmental adaptation; and 2) do beneficial genetic mutations occur and are they retained in the population? Some studies have combined random mutagenesis and domestication into one experiment [28,31], adding to the confusion of mechanism analysis.

To clarify the action mechanism of CO_2 gradient domestication on microalgal tolerance and growth ability in the presence of high CO_2, this study performed gradual gradient acclimation of CO_2 using wild-type *Nannochloropsis oceanica* CCMP1779 and carried out a comprehensive combined analysis of the genome, transcriptome, photosynthetic fluorescence and RT-qPCR. It was revealed that functionally selective multi-target gene mutations were caused by the CO_2 gradient domestication process on microalgae, thereby improving photosynthesis, carbon fixation and cell synthesis. Finally, cultivation under a high and moderate

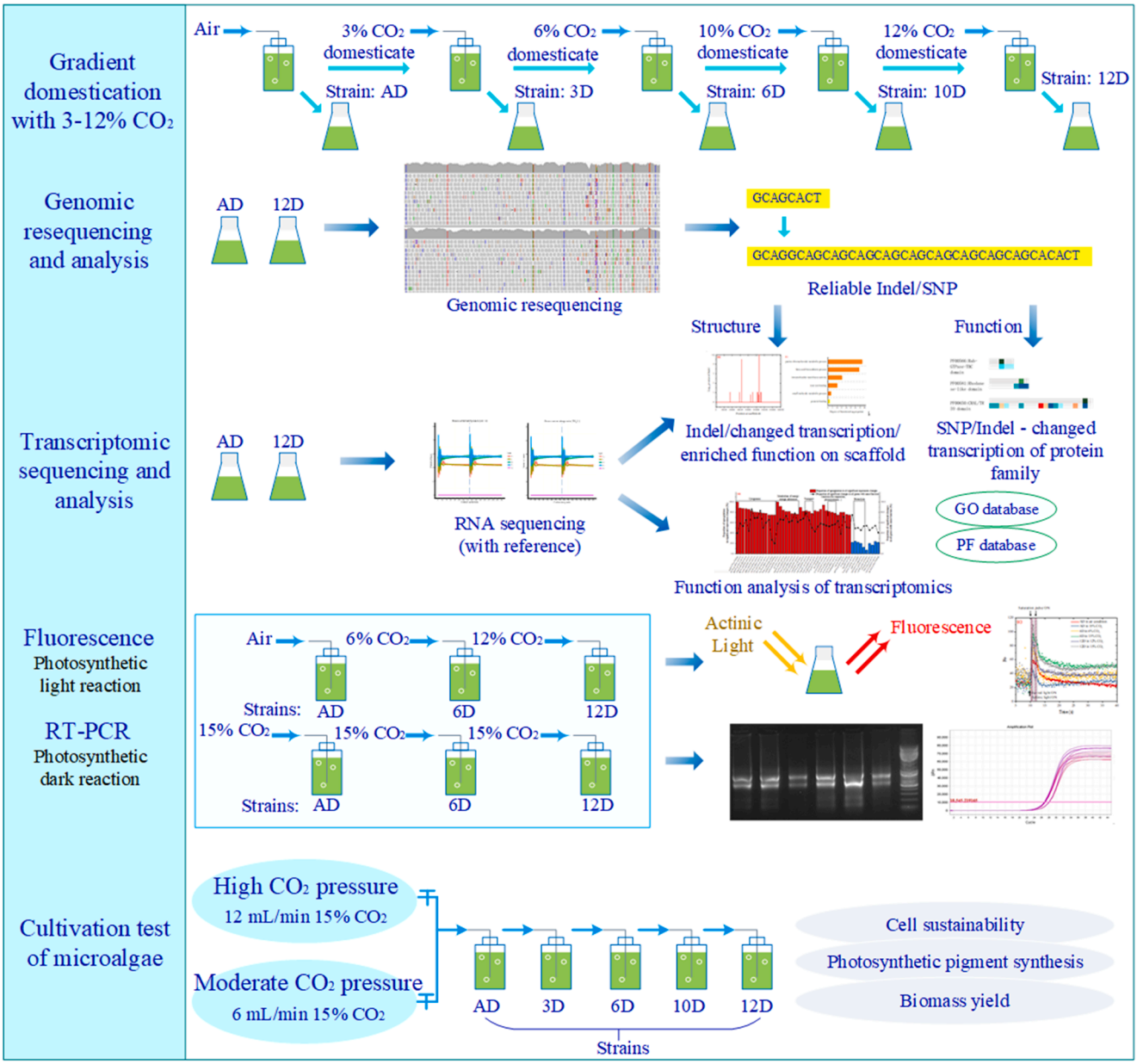

Fig. 1. Research methods on adaptive laboratory evolution of microalgae cultivated with high concentrations of CO_2.

flow rate of 15% CO_2 showed the superiority of gradually domesticated microalgal strains, which exhibited higher biomass yield, photosynthetic pigment content and survival. Thus, this study demonstrates the mechanism, significance and applicability of using CO_2 gradient domestication to obtain effective microalgal strains for cultivation with high CO_2 concentration flue gas.

2. Experimental methods

2.1. Gradual domestication with high CO_2 concentration for microalgae

The research method to identify the promoting mechanism involved in gradual domestication of microalgal tolerance to high CO_2 concentration is shown in Fig. 1. Gradual acclimation was carried out with a CO_2 gradient from 0.04% (air) to 12% CO_2 to obtain domesticated strains of *N. oceanica* CCMP1779. The gene mutations produced by adaptive laboratory evolution were investigated by genomic resequencing of the control (AD) and domesticated (12D) strains, while transcriptomic sequencing was conducted to detect the differential gene expression profiles between AD and 12D. After data filtering and analysis of the genomic results, reliable indel and SNP mutations (p-value $<$ 0.05 & FDR $<$ 0.05 & increased allele frequency in 12D) that occurred during the process of domestication were assigned as the baseline for the associated analysis of genomics and transcriptomics. The joint analysis mainly included two aspects: 1) for the scaffolds with reliable indel mutation aggregation, the extensive distribution of indels induced by reliable indel mutations on the scaffolds, the significant changes of gene expression on the scaffolds caused by extensive mutation, and the functional classification statistics of these genes were analyzed; and 2) the protein families of genes directly related to reliable SNP and indel mutations were traced upward to analyze the occurrence of reliable gene mutations and differences in transcription levels within the protein families. Differences in transcriptome expression directly caused by genome mutations were clarified by the above two factors. Next, functional statistics of the significant expressional differences between the AD (control) and 12D (domesticated) groups were performed to reflect the overall transcription differences further linked to the transcriptome differences caused by the above gene mutations.

To further clarify the effect of CO_2 gradient acclimation on the photosynthetic carbon sequestration mechanism of microalgae, photosynthetic fluorescence and RT-qPCR were used to measure the light reaction and dark reaction of microalgal strains during each stage of acclimation (AD, 6D, 12D) and those under high carbon conditions (6 mL/min 15% CO_2). Photosynthetic fluorescence analysis included determining the photosynthetic electron transfer rate, photosynthetic system recovery against saturated light, non-photochemical quenching and cyclic electron transport. RT-qPCR included analysis of key enzymes involved in the inorganic carbon ion balance, carbon transport, C4 process and Calvin cycle. Finally, to test the macroscopic growth effect of *N. oceanica* CCMP1779 after adaptive laboratory evolution for CO_2 gradient domestication, the strains obtained from each domestication stage (AD, 3D, 6D, 10D, 12D) were cultivated in two high CO_2 environments (high pressure: 12 mL/min 15% CO_2; moderate pressure: 6 mL/min 15% CO_2). The high pressure condition was mainly set to reflect the survival ability of the microalgal strains against CO_2, while the moderate pressure condition was set to reflect the photosynthetic growth and biomass productivity of microalgal strains under high CO_2 concentration flue gas.

2.2. Adaptive laboratory evolution of the wild-type microalgal strain

Wild-type *N. oceanica* CCMP1779, a unicellular microalga, was used as the experimental strain in this study. For every stage of the whole experiment, seawater culture medium, consisting of artificial seawater (ESAW Medium) and optimized f/2 medium [29], was chosen as the only cultivation medium for the microalgae. Photoreactors for *N. oceanica* cultivation were made up of a series of 300-mL column bioreactors of 160 mm height, 56 mm inner diameter and 62 mm outer diameter. The photoreactors were kept in an artificial greenhouse where the temperature and light were maintained at 25 °C and 55 $\mu mol \cdot m^2 \cdot s^{-1}$. To speed up the growth process, a dark/light cycle was no implemented.

To promote a tolerance to high CO_2 concentrations, wild-type domesticated microalgal strain *N. oceanica* CCMP1779 was gradually acclimated to a CO_2 gradient. This acclimation included five stages with a gradually increasing proportion of CO_2 in the injection gas: 1) ambient concentration; 2) 3% CO_2/97% N_2; 3) 6% CO_2/94% N_2; 4) 10% CO_2/90% N_2; and 5) 12% CO_2/88% N_2. The gas flow rate to each photoreactor was controlled by an electric flow meter at 30 mL/min. During each stage, 3 cultivation cycles of 8 days each were included. At the beginning of each cycle, the initial inoculation concentration of *N. oceanica* CCMP1779 in the photoreactors was $OD_{750} = 0.3$. To further study changes in the microalgae caused by gradient acclimation to CO_2 gas, a portion of the microalgae was stored in an incubator with constant temperature of 25 °C and light of 55 $\mu mol \cdot m^2 \cdot s^{-1}$ (without dark/light cycle) at the end of each stage. The resulting domesticated strains were named based on the final CO_2 concentration to which they were exposed, specifically AD (ambient air cultivation), 3D (two-stage domestication with ambient air and 3% CO_2), 6D (three-stage domestication with ambient air, 3% CO_2 and 6% CO_2), 10D (four-stage domestication with ambient air, 3% CO_2, 6% CO_2 and 10% CO_2) and 12D (five-stage domestication with ambient air, 3% CO_2, 6% CO_2, 10% CO_2 and 12% CO_2). Several parallel photoreactors were prepared in this step.

2.3. Genomic resequencing and data filtering

Several samples (2 AD samples and 4 12D samples) were collected randomly from the constant temperature and light incubator. Each sample represented about 0.2 L of microalgal suspension and 10^9-10^{10} *N. oceanica* CCMP1779 cells. DNA was extracted based on the CTAB method. DNA samples were randomly broken into 350 bp fragments by the Covaris crusher (S220, Covaris, USA), which were then used to build the library with the TruSeq Library Construction Kit (Novo, Denmark). After preparation via end repair and phosphorylation, adding A-tails, ligating index adapters, denaturation and amplification, the DNA library for each sample was constructed followed by quantification with Qubit 2.0 (Invitrogen, USA) and finally diluted to 1 ng/μL. After the expected insert size was obtained, the effective concentration of the library was accurately quantified by qPCR to ensure the library quality. The effective concentration of the library was determined as $>$ 2 nM. The library was sequenced by Illumina HiSeq (NovaSeq 6000, Illumina, USA) to obtain the original image data files, which were converted into sequenced reads (raw data) by base calling analysis. The raw data was filtered to exclude paired-end reads with a ratio of N in the single-end sequencing reads exceeding 10% of the read length, a ratio of low quality bases ($Q \leq 5$) in single-end sequencing read exceeding 50% of the read length, and with adapters. The effective sequencing data were compared to the reference genome using BWA software (parameter: mem-t 4-k 32-m), and the annotated results with the reference genome were removed by SAMTOOLS (parameter: rmdup). For all SNPs and indels, the filter standard (including DP >= 4 & MQ >= 20) was enforced to obtain high-quality data from each sample for further analysis. The basic quality information from the gene resequencing is listed in Table S1 in Supplementary File 1. For the genomic resequencing conducted in this study, the reference genome of *N. oceanica* CCMP1779 (https://mycocosm.jgi.doe.gov/Nanoce1779_2/Nanoce1779_2.info.html) was obtained from the U.S. Department of Energy Joint Genome Institute (DOE JGI), which was contributed by Yasuo Yoshikuni at the DOE JGI and Krishna Niyogi at the University of California Berkeley. Usage permission was obtained before use.

2.4. RNA sequencing and data filtering

After domestication, activation cultivation was conducted for two days under 6 mL/min 15% CO_2 to collect AD and 12D (2 samples each) for mRNA extraction and library construction. RNA was extracted from the samples using the TRIzol method. A total of 1 μg RNA per sample was used as input material for RNA sample preparation. Sequencing libraries were generated using the NEBNext UltraTM RNA Library Prep Kit (NEB, USA) for Illumina following manufacturer's recommendations and index codes were added to assign sequences to each sample. Briefly, mRNA was purified from total RNA using poly-T oligo-attached magnetic beads and then the cDNA was synthesized for library construction. Clustering of the index-coded samples was performed on a cBot Cluster Generation System using the TruSeq PE Cluster Kit v3-cBot-HS (Illumina, USA) according to the manufacturer's instructions. After cluster generation, the library preparations were sequenced on the Illumina NovaSeq platform (NovaSeq 6000, Illumina, USA) and 150 bp paired-end reads were generated as raw data.

Raw data in fastq format were first processed through in-house Perl scripts. In this step, clean data (clean reads) were obtained from the raw data by removing reads containing adapters and poly-N sequences, as well as low quality reads. At the same time, Q20, Q30 and GC content of the clean data were calculated. All downstream analyses were based on the high-quality clean data.

Clean paired-end reads were aligned to the *N. oceanica* CCMP1779 reference genome of using Hisat2 (v2.0.5). The mapped reads for each sample were assembled by StringTie (v1.3.3b) [51] using a reference-based approach. FeatureCounts (v1.5.0-p3) was used to count the read numbers mapped to each gene. Next, the fragments per kilobase of exon per million reads mapped (FPKM) of each gene was calculated based on the length of the gene and read counts mapped to the gene. The AD samples were set as the control group and the 12D samples as the domesticated group, then the differential gene expression profiles between the groups were obtained using the DESeq2 package (v1.16.1). In this research, the standard for a significant change in gene expression was always a p-value < 0.05. The basic quality information for the transcriptomics is listed in Table S1 in Supplementary File 1.

2.5. Association analysis between the genome and transcriptome

Before analysis, all the genes were annotated with the clusterProfiler package in R [23] against the PF (Protein Family), GO (Gene Ontology) and KEGG (Kyoto Encyclopedia of Genes and Genomes) databases, the results are shown in Supplementary File 3. Consolidation of genomic data from control and domesticated samples was conducted to clarify the significant mutations that occurred during the process of CO_2 gradient acclimation, so reliable indels and SNPs were filtered based on the following standards: p-value < 0.05, FDR < 0.05 and average allele frequency in domesticated samples $>$ average allele frequency in control samples. Additionally, SNP entries with ≤ 200 bp distance to the nearest reliable indel were neglected. The filtered results are listed in Table S2 in supplementary File 1.

Because of the important role played by indels in natural evolution [16], reliable indels and their corresponding indel mutations were subjected to statistical analysis based on the p-value of the enriched reliable indels on the scaffold. In total, 305 scaffolds in *N. oceanica* CCMP1779 were ranked according to their chi-square test p-value with the proportion of reliable indels on the scaffold to the total reliable indels and genes on the scaffold. The smallest 5% of the total scaffolds were selected. Additionally, the successful association effect of reliable indels on transcriptional expression was set as another filter standard for scaffolds selection. Thus, only scaffolds with an absolute value of an average $\log_2$ fold change of the FPKM of all genes higher than 0.3 were retained as a scaffold with successful association in the following analysis. For those retained scaffolds, all indels satisfying the standard that the average allele frequency of the domesticated groups – the average allele frequency of wild-type groups ≥ 0.5 were listed as associated indels occurring with the reliable indel. Accordingly, all genes with a significant change in expression on these scaffolds were categorized for their function using the GO database. To evaluate the influence of reliable indels on physiological function, the average $\log_2$ fold change of the FPKM and the "degree of functional aggregation" index were calculated for each function on one of the scaffolds (Eqn. (1)).

$$degree\ of\ functional\ aggregation(function: A,\ scaffold: B) = \frac{F_A S_B}{F_A} \Big/ \frac{F_A}{T} \quad (1)$$

Here, F_AS_B represented the amount of significant changed expression genes within function A on scaffold B, S_B represented the amount of significant changed expression genes on scaffold B, F_A represented the amount of significant changed expression genes within function A and T represented the amount of significant changed expression genes.

To produce a more meaningful analysis, only entries with a degree of functional aggregation > 4 were retained when discussing functional aggregation of the various scaffolds.

The functional entries with significant changes in their transcriptional level occurring in each one of those remaining scaffolds after filtration were listed as the function with a co-occurrence change in transcriptional expression and their average degree of functional aggregation was calculated.

Another analysis was related to the detailed position of reliable SNPs and indels and describes the function affected by the mutation in detail. Because SNPs and indels occurring in a certain position may affect the transcriptional expression of one or two closely related genes, all reliable mutations and significant changes in the transcriptional expression of genes of a protein family were collected and displayed in a heat map named by their PF entry. The significantly promoted or inhibited protein family obtained an average $\log_2$ fold change > 0.5 or average $\log_2$ fold change < -0.5.

2.6. Functional analysis of the transcriptome

Transcriptomic analysis was based on the GO and PF annotations related to genes with significant up-regulation or down-regulation. For each functional entry three indexes were calculated: the proportion of up-regulation in the total significantly changed genes with the same function; the proportion of significantly changed genes in the total genes with same function; and the average $\log_2$ fold change. The functional entries in the GO groups were filtered based on the standard that that first index was $> 75\%$ or $< 25\%$, which were considered as a significant up-regulation of function and significant down-regulation of function, respectively. The functional entries in the PF groups were filtered based on the standard that the second index was $\geq 50\%$ and the average $\log_2$ fold change ranked as positive or the penultimate 10%, which were also considered as a significant up-regulation of function and a significant down-regulation of function, respectively. In this analysis, the entries with exactly the same genes were merged and only one entry was kept that could clearly depict the function to prevent too many similar entries disturbing the results.

2.7. Photosynthetic fluorescence measurement

In this study, photosynthetic fluorescence was measured to evaluate changes to the photosynthetic light reaction during the process of CO_2 gradient acclimation using an FMS-2 (Hansatech, United Kingdom) with a 594 nm light source. Strains AD, 6D and 12D were selected as the experimental strains. One data set was collected under the original cultivation environment of the strain to represent the photosynthetic light system gained in different stages of domestication, for example AD with 30 mL/min air, 6D with 30 mL/min 6% CO_2 and 12D with 30 mL/min 12% CO_2. Another data set for AD, 6D and 12D was collected with 6

mL/min 15% CO_2 to test the ability of the photosynthetic light reaction of the domesticated microalgal strains under the high CO_2 stress.

Rapid light curves [43] were constructed by measuring the effective quantum yield of photochemical energy conversion in PS2 (ΦPSII) with gradually decreasing light intensity, specifically 2000, 1482, 1190, 1015, 800, 603, 390, 204, 104, 70, 46, 20, 10 and 0$\mu mol{\cdot}m^{2}{\cdot}s^{-1}$. The adaptive time for each stage was 4.5 min, then a 2.5 s saturated pulse was illuminated to measure the ΦPSII value. The relative effective photosynthetic electron transport rate (rETR) of every light intensity stage was calculated using Eqn. (2) [45]:

$$[rETR]\mu mol{\cdot}m^{-2}{\cdot}s^{-1} = ([PFD]\mu mol{\cdot}m^{-2}{\cdot}s^{-1}) \times (\Phi PSII) \times 0.5 \times 0.84 \quad (2)$$

where rETR represents the relative effective photosynthetic electron transport rate; PFD represents the actual luminous flux density; and ΦPSII represents the effective quantum yield of the PSII photochemical energy conversion. For each experimental object, the PFD and associated rETR were fitted by Eqn. (3) to obtain the rapid light curve:

$$rETR = \frac{PFD}{a{\cdot}PFD^{2} + b{\cdot}PFD + c} \quad (3)$$

Three main indexes were obtained from the fitted rapid light curve, namely the maximum relative photosynthetic electron transfer rate ($rETR_{max}$), representing the maximum rETR value on the curve; the half-saturation light intensity (I_k), representing the corresponding PFD value when the rETR was half of the extreme value; and the initial slope (α), representing the slope at the beginning of the curve.

Another trial was then conducted to test the recovery ability and momentary light protection ability against strong light by observing the response to a continuous saturation pulse. In this test, after 10 min of dark adaptation, far red light was used to activate the PSI system. At the same time, a 0.8 s saturated pulse was illuminated to obtain the first peak. After 0.8 s recovery in the dark, another 0.8 s saturated pulse was illuminated to obtain the second peak. Based on the fluorescence value gathered by the FMS-2 instrument, the curves were smoothed using the Haar wavelet type and Lowess method to reduce the fluorescent noise from aquatic organisms. The following three indexes were calculated to better depict the momentary light protection that occurred in this process: the fluorescence recovery amount at the secondary pulse occurrence point (F_{PS}; Eqn. (4)); the fluorescence recovery ratio at the secondary pulse occurrence point (ΦPS; Eqn. (5)); and the ratio of the secondary peak to the primary peak (ΦS; Eqn. (6)). The fluorescence value of the curves was F(t) at each time point t.

$$F_{PS} = F(t_{P1}) - F(t_s) \quad (4)$$

$$\Phi PS = \frac{F_{PS}}{F(t_{P1}) - F(t_o)} \quad (5)$$

$$\Phi S = \frac{F(t_{P2}) - F(t_s)}{F(t_{P1}) - F(t_o)} \quad (6)$$

Where t_o represents the time point when the primary saturated pulse begins illumination; t_{p1} represents the time at which the primary peak is highest during illumination of the primary saturated pulse; t_s represents the time point at which the secondary saturated pulse begin illumination; and t_{p2} represents the time at which the secondary peak is highest during illumination of secondary saturated pulse.

The fast and slow phases of non-photochemical quenching (NPQ) were measured on a larger timescale to represent the light protection ability. The measurements started from 20 min dark adaptation and then a saturated pulse was illuminated to obtain the Fm value. Next, a strong actinic light was used for 10 min of light adaptation and then a saturated pulse was illuminated to obtain the Fm' value. Then the actinic light was turned off to start a recovery process against strong light damage during 30 min. The final Fm' value, referred to as $F^{t}m$, was obtained after this process. The fast and slow phases of NPQ were calculated using the following formula (Eqn. 7) [43]:

NPQ (fast phase) = (Fm/ Fm')-(Fm/ $F^{t}m$) (7)

NPQ (slow phase) = (Fm-$F^{t}m$)/$F^{t}m$ (8)

The measurement for NPQ was conducted under two actinic light intensities: 1200$\mu mol{\cdot}m^{2}{\cdot}s^{-1}$ and 800$\mu mol{\cdot}m^{2}{\cdot}s^{-1}$.

Finally, a test for PSI, named post-illumination, was conducted according to previous literature [60,79]. After 5 min of light adaptation with 800 $\mu mol{\cdot}m^{2}{\cdot}s^{-1}$ actinic light and far red light, a sudden decrease of fluorescence occurred when the actinic light was turned off. It then gradually recovered within 10 s. The slope of this increase from the lowest point of the flop to the instantaneous peak was calculated to represent the cyclic electron transport rate around PSI.

2.8. RT-qPCR for carbon transport and photosynthetic dark reaction

The transcription levels of 16 genes were selected to comprehensively evaluate the influence of CO_2 gradient acclimation on the photosynthetic dark reaction. These 16 genes were selected according to the genome and gene models of *Nannochloropsis oceanica* CCMP1779, which was sequenced by the laboratory of Christoph Benning at Michigan State University (https://mycocosm.jgi.doe.gov/Nanoce1779/Nanoce1779.info.html), because the function of these enzymes has been reported in the corresponding literature [3].

Enzymes related to carbon fixation can be mainly divided into three parts: transport and intracellular stabilization of CO_2; photosynthesis (including light and dark reactions); and the C4 mechanism so-called "temporary storage for CO_2". The key enzymes selected in this study were completely covered by these three parts. First, two carbonic anhydrases (*CAH-1* and *CAH-2*), as well as the inorganic carbon transmembrane transport enzymes carbonate counter pump (*CCP*) and Limiting CO_2 Inducible A (*LCIA*), were measured to reflect inorganic carbon transport and carbon ion equilibrium, the prophase of the dark reaction. Second, key enzymes in the C4 process were measured to reflect the carbon storage capacity that assists the dark reaction, including two pyruvate, phosphate dikinases (*PPDK-1* and *PPDK-2*); three malate dehydrogenases (*MDH-1*, *MDH-2* and *MDH-3*); two malic enzymes (*ME-1* and *ME-2*); and a phosphenolpyruvate carboxylase (*PePcase*). Finally, the core ribulose-1,5-bisphosphate oxygenase (RuBisCO) isoenzymes *rbcS*, *rbcL-1*, *rbcL-2* and *rbcL-3* were measured to determine the carbon fixation capacity of the Calvin cycle. In this experiment, each enzyme covered all isoenzyme genes previously reported in the literature [3]. Moreover, two 18S rRNA genes (*18S-1* and *18S-2*) were also measured as two internal references to ensure data reliability. Detailed model names from the genomic database and their primer sequences are listed in Table S3 in Supplementary File 4.

In this research, AD, 6D and 12D were selected as the experimental strains. One data set was collected under the original cultivation environment to represent the photosynthetic dark system gained during different stages of domestication, for example AD with 30 mL/min air condition, 6D with 30 mL/min 6% CO_2 and 12D with 30 mL/min 12% CO_2. Another data set for AD, 6D and 12D was collected with 6 mL/min 15% CO_2 to test the ability of the photosynthetic dark reaction for domesticated microalgal strains under high CO_2 stress. All samples were collected during the logarithmic growth period at an OD_{750} between 0.8 and 1.4.

Total RNA was extracted using a UNIQ-10 Column Trizol Total RNA Extraction Kit from Sangon Biotech Co., Ltd (Shanghai, China). Reverse transcription was performed using a fluorescent quantitative PCR instrument (StepOnePULS, USA) to obtain cDNA. Samples were diluted ten-fold for use as template cDNA with corresponding primers. PCRs were performed for 45 cycles using the fluorescent quantitative PCR instrument. Data were analyzed as relative expression levels ($-\Delta\Delta C_T$); the AD group (cultivated with air) was selected as the baseline. To clearly assess the transcriptional expression of key enzymes that possess multiple isozyme genes, a "pseudo relative expression level", which was calculated by combining the expression levels of each isoenzyme, was used as analytical evidence for clearer evaluation. Specifically, for every

key enzyme consisting of multiple isozyme genes, and for each sample, the ΔC_T of the isoenzyme genes were added up as the ΔC_T of this "pseudo relative expression level". The $-\Delta\Delta C_T$ was calculated with the baseline of the AD group.

2.9. Cultivation tests for gradually domesticated N. Oceanica under 15% CO_2

Two independent cultivation tests for *N. oceanica* strains in different stages of CO_2 gradient domestication for high CO_2 tolerance were conducted under two 15% CO_2 gas aeration rates: 6 mL/min and 12 mL/min. According to experimental experience, the survival of *N. oceanica* CCMP1779 in little>6 mL/min 15% CO_2 gas is low; therefore, the likelihood of survival under 12 mL/min 15% CO_2 would be lower. Accordingly, these two aeration rates were selected to represent relatively moderate and extreme pressure conditions to test the significance of CO_2 gradient acclimation on microalgal growth.

In each set of independent experiments, AD, 3D, 6D, 10D and 12D were cultivated from an initial microalgal concentration $OD_{750} = 0.2$ with artificial seawater (ESAW medium) and optimized f/2 medium [29]. Photoreactors for cultivation (a series of 300-mL column bioreactors) were same as those used in cultivation. The artificial greenhouse conditions were also the same as stated in section 2.2. Two parallel experiments were conducted for each microalgal strain.

During cultivation, 10 mL of microalgal suspension were randomly harvested and their OD_{750} value was measured. Next, the samples were dewatered via centrifugation and then washed three times with deionized water. The pellet was collected and the subsequent biomass was measured after drying at 80 °C for 72 h. Because of the linear relationship between the biomass yield and OD_{750}, the calculated microalgal biomass dry weight was obtained by fitting and the biomass yield for each day was calculated with this formula.

Additionally, during cultivation, the pH of microalgal suspension was measured daily using a pH meter (Mettler Toledo, FE20, Switzerland). No manual pH adjustments were conducted in this study.

Due to the common occurrence of cell death, the proportion of viable cells was measured for the 12 mL/min 15% CO_2 experiment on the 6th day of cultivation using the neutral red method [17]. The survival proportion was based on the results of both the colorimetric method and by electron microscope observations.

For the experiment with 6 mL/min 15% CO_2, the chlorophyll and carotenoid contents of *N. oceanica* CCMP1779 were measured daily by spectrophotometry. Briefly, after collecting 1 mL of microalgal suspension via centrifugation, 3 mL of anhydrous methanol (>99.9%) was added to the pellet and evenly mixed. After 15 min of dark treatment, the absorbance values A_{652}, A_{665} and A_{480} of the supernatant were measured using a spectrophotometer (Thermo Scientific, USA). If the absorbance was > 1.0, the supernatant was diluted until it was < 1.0.

Chlorophyll *a* (Chl-a) and carotenoids were measured in this experiment because chlorophyll *b* is not contained in *N. oceanica*. The calculations were as follows [25,64]:

$$[\text{Chl-a}]\ \mu g\ mL^{-1} = -8.0962 \times A_{652} + 16.5169 \times A_{665} \quad (9)$$

$$[\text{Carotenoids}]\ \mu g\ mL^{-1} = 4 \times A_{480} \quad (10)$$

3. Results

3.1. Extensive transcription differential linkage induced by enrichment of indel mutation in CO_2 gradient domestication

There is a deeply held hypothesis that indels play an important role in evolution as a source of genetic variation, because they contribute to base changes in the surrounding coding regions [16]. This mechanism is referred to as IDAM (indel-associated mutation) in previous studies [39]. Therefore, reliable indels and their associated changes in transcriptional levels were selected as the primary entry point for CO_2 gradient acclimation-induced gene mutation and species evolution. After filtration with the standards outlined in section 2.5, four scaffolds in *N. oceanica* CCMP1779 stood out from the total 305 scaffolds because they exhibited the most aggregated reliable indel mutations and successful association in transcriptional changes (Fig. 2). In these four scaffolds, a series of indels with low reliability were identified around the reliable indels, which almost never occurred in the control group but occurred with large probability (p-value < 0.05 & FDR < 0.05) as a homozygote in the domesticated group. One hypothesis for this is that the indel with low reliability is secondary, unstable and random, but there is no doubt that individuals with these indel mutations under the CO_2 gradient cultivation also gained some natural selection advantages because the allele frequency of these indels was significantly increased from the control group to the domesticated group. Mutations that could be passed down from a population were widespread around reliable indels in the domesticating group, which demonstrates that species evolution was induced by CO_2 gradient acclimation.

In the theory of IDAM, indels with wide distribution in non-coding regions contribute to a high rate of evolution for gene expression [16]. In this study, a large number of genes on the same scaffold showed significant changes in expression ($p < 0.05$) due to indels. The function of genes with expression changes are summarized in Fig. 2(i)-(m). The significant common functions exhibiting up-regulated expression on the four scaffolds were phosphate-containing compound metabolism and oxidoreductase activity. The former is closely related to synthesis and metabolism of phosphoribose and deoxyphosphoribose, which constitute genetic material; thus, this up-regulation may promote the activity of genetic transcription and cell construction. The latter is widely involved in cellular photosynthesis and respiration. On the contrary, the common function exhibiting down-regulated expression on the four scaffolds was hydrolase activity, which may inhibit proteolysis in the domesticated cells. Active cell construction, enhanced accumulation and depletion of energy-storing substances, and more stable proteins are the primary characteristics of extensive genetic mutations associated with indel mutations during domestication of cells. The above tendency was also reflected in the function statistics of genes possessing significant changes on each scaffold, such as the significant up-regulation of the purine ribonucleoside metabolic process (related to genetic material), fatty acid biosynthesis (related to carbon accumulation), phospholipid binding (related to biofilm construction), oxidoreductase activity acting on NAD or NADP (associated with photosynthesis or respiration) and generation of precursor metabolites and energy. Meanwhile, significant down-regulation occurred for threonine-type endopeptidase activity (involved in proteolysis), transcriptional repressor complex (inhibits transcriptional processes) and flavin adenine dinucleotide binding (related to the FAD pathway of respiration).

Additionally, the main three electron transport chains in microalgal cells showed some differentiation, NADP (photosynthesis) and NAD (one pathway of respiration) were promoted, while FAD (one pathway of respiration) was inhibited. Similar differentiation also occurred for ion binding in that genes related to binding of the iron ion were up-regulated but genes related to binding of the magnesium ion were down-regulated. The smooth binding of iron ions is helpful for the assembly of chlorophyll synthesis catalytic enzymes, thereby promoting chlorophyll synthesis and photosynthesis. The slight down-regulation of the magnesium ion binding enzyme may maintain sufficient free magnesium ions to promote stacking of the photosynthetic chloroplast membrane [27] and ensure activity of key enzymes in the photosynthetic dark reaction [24]. However, as a side effect of widespread mutations, cell redox homeostasis, including some antioxidant activity, may be weakened to a certain degree. This may dwarf the ability of domesticated cells to defend against toxins in the environment [68].

3.2. Functionally directed SNP and indel mutations: Induced transcriptional differences in CO_2 gradient acclimation

Mutations may directly change the expression or function of closely

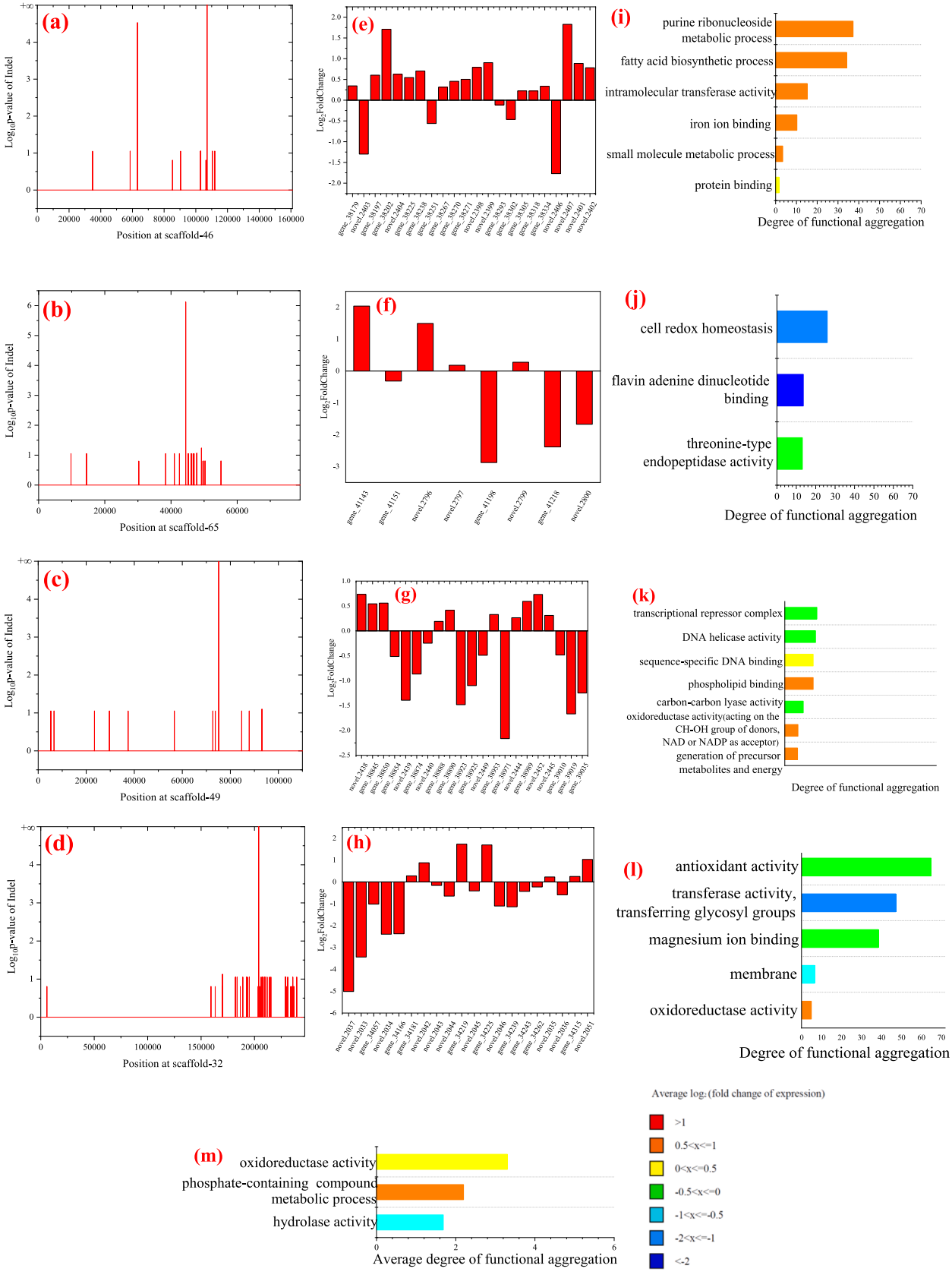

Fig. 2. Extensive transcription differential linkage induced by enrichment of Indel on scaffolds of CO_2 domesticated *N.oceanica* strains. Indels on (a) scaffold-46, (b) scaffold-65, (c) scaffold-49, and (d) scaffold-32. Genes with significant transcriptional differences (p-value < 0.05) on (e) scaffold-46, (f) scaffold-65, (g) scaffold-49, and (h) scaffold-32 (sort by base positions on the scaffold). Main functional clustering of genes with significant differences on (i) scaffold-46, (j) scaffold-65, (k) scaffold-49, (l) scaffold-32 and (p) co-occurrence.

associated genes, which leads to differences in species traits [50,62]. Because of the possible associated changes that happened in genes within the same protein families owing to connections and interactions between similar functional enzymes, the influence of SNPs and indels on one gene may spread to all genes in the same protein family. Moreover, the enzymes within one protein family would play a similar physiological role in the microalgal cells, so the influence of SNPs and indels on a certain function should be evaluated with all the genes of a protein family. To fully evaluate the effect caused by gene mutation, the protein family of the gene directly associated with reliable SNPs and indels (within one gene or between the two genes in which the mutation occurred), and the reliable mutation and significant expression difference of similar genes within the same protein family were visualized in the form of a heat map (Fig. 3). These genes showed a strong categorization in function and were thus classified into six broad groups, namely light response, transporter, sugar metabolism, cytogenesis, respiration and proteolysis. Accordingly, they showed a prominent aggregation to light reaction, metabolism and biosynthesis of energy storage materials, as well as cell construction.

Not all mutations led to efficient association at the transcriptional level. Therefore, those protein families that successfully interlink at the transcriptional level from mutation are particularly noteworthy. The most noticeable category was “light response” because all the protein families contained a reliable mutation, thereby successfully inducing widespread significant up-regulation at the transcriptional level. The protein family PF02514/PF11965 included 2 genes detected throughout this experiment, which were assigned to the KEGG pathway of porphyrin and chlorophyll metabolism as key enzyme magnesium chelatase (EC 6.6.1.1), based on alignment of the domain. From the KEGG database, the synthesis of chlorophylls and cytochrome *c* share the same metabolic pathway. The starting compound is protoporphyrin IX, but the process branches depending on the regulation by one of two key enzymes: protoporphyrin ferrochelatase (EC 4.99.1.1) catalyzes protoporphyrin IX into the cytochrome synthesis pathway [40,55], while magnesium chelatase (EC 6.6.1.1) catalyzes it into the chlorophyll synthesis pathway [18]. Cytochrome *c* plays an essential role in oxidative phosphorylation within the mitochondria during cellular respiration, but chlorophyll is the basis for the whole photosynthetic light reaction. Because of direct competition between the synthesis of chlorophyll and cytochrome *c*, gene mutation and the resulting up-regulation of magnesium chelatase (EC 6.6.1.1) means that protoporphyrin IX was selectively converted to Mg-protoporphyrin IX, an intermediate in chlorophyll synthesis [4], which guaranteed the dominance of photosynthesis in the physiological and metabolic activities of domesticated cells. At the same time, other genes related to photoresponsive function also exhibited similar mutations and an associated increase in

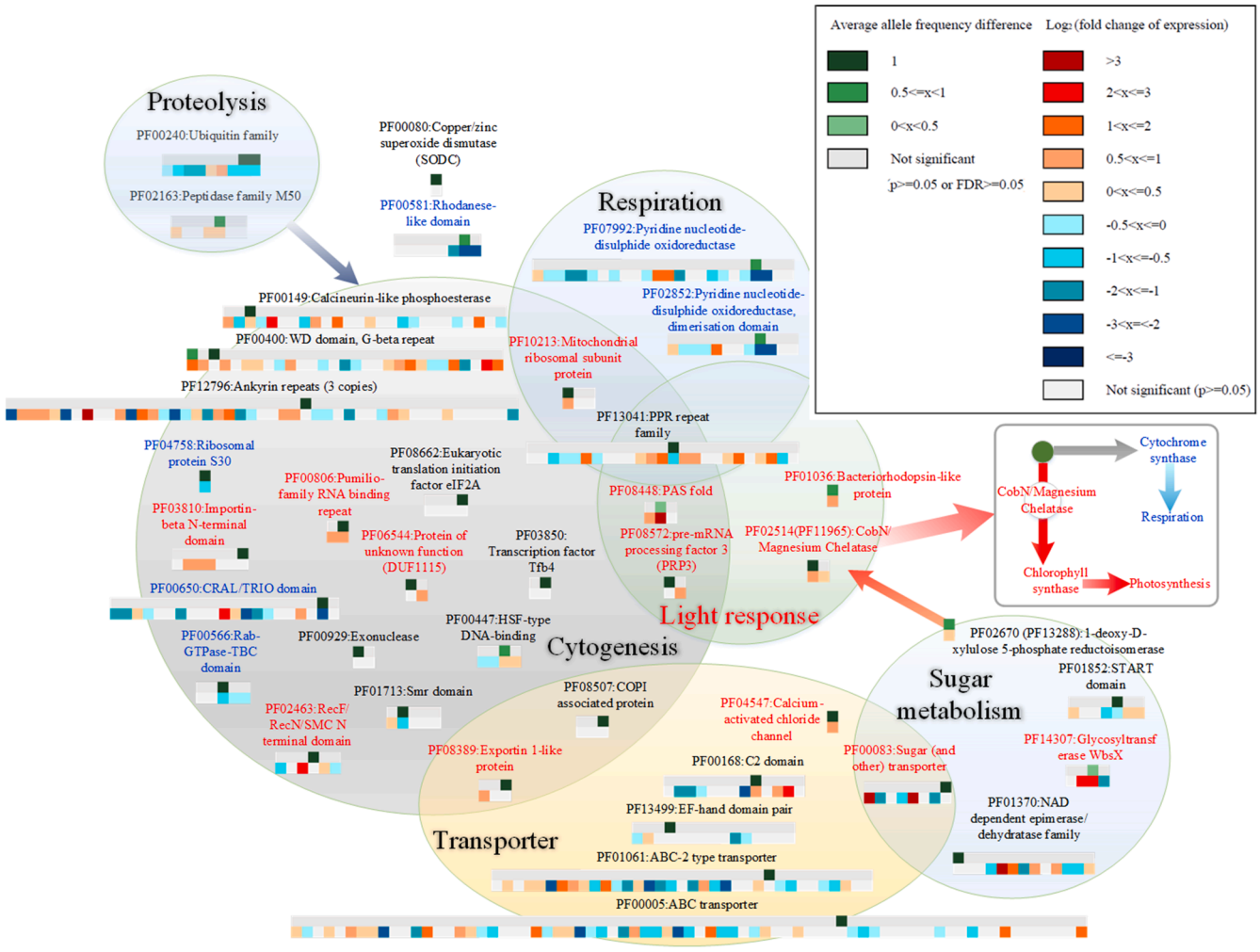

Fig. 3. Functional enrichment of reliable SNP and Indel (p-value < 0.05 and FDR < 0.05) and changes in transcriptional expression of related genes within the same protein families. The first line for each protein family in heat map represents gene mutation (using different greens to indicate the size of average allele frequency difference), and the second line represents transcriptional expression (using different reds to indicate the up-regulated $\log_2$ fold change and different blues to indicate the down-regulated $\log_2$ fold change). The PF name indicated by red represents a significant up-regulation of this protein family (average $\log_2$ fold change > 0.5), and also blue represents a significant down-regulation (average $\log_2$ fold change < -0.5).

transcription, such as PF01036, PF08572 and PF08448. Genes in the protein family PF01036 are rhodopsins found in archaea, bacteria and fungi, and they provide light-dependent ion transport and sensory functions to halophilic microorganisms [2,15]. Genes in the protein family known as pre-mRNA processing factor 3 (PRP3) are mainly found in yeast and humans, and they induce photoreceptor degeneration in retinitis pigmentosa due to a missense mutation [9]. Although their role in photosynthetic microalgae has not been studied, PRP3 is considered an important part of the light-sensing system, and it can be hypothesized that they are closely related to a physiological process that cooperates with photosynthesis under light conditions. Furthermore, PF08448, known as the PAS domain, is widespread and associated with many signaling proteins as a signal sensor domain to transduce redox signals and regulate circadian rhythms by sensing oxygen, redox potential or light [8]. Thus, the PAS domain may also have important significance for the regulation of photosynthesis.

In addition to the substantially improved light response, some protein families closely related to sugar metabolism also showed concentrated mutations and a corresponding transcriptional up-regulation. As a necessary pathway for the utilization of photosynthetically fixed carbon, the spontaneous editing of genes for sugar metabolism may mean that the cell needs a more vigorous carbon utilization process to compensate for the vigorous photosynthesis. For example, most members in PF00083 are sugar transporters for transport of various carbohydrates [56], while PF14307 represents a series of glycosyltransferases [36]. Furthermore, a slight up-regulation in PF02670, represented by 1-deoxy-D-xylulose-5-phosphate reductoisomerase (EC 1.1.1.267) [69], may have some significance in photosynthetic pigment synthesis because it is the key enzyme in the MEP/DOXP pathway for terpenoid biosynthesis, which is the cohesion process between glycolysis and carotenoid biosynthesis. Thus, it is a necessary step for converting photosynthetically fixed carbohydrates to geranylgeranyl pyrophosphate and farnesyl pyrophosphate, which are the starting compounds for carotenoids synthesis, according to the KEGG database.

Another large group for reliable mutations was cytogenesis, mainly including DNA processes, transcription and protein construction. This may indicate that cell building processes, such as translation and transcription, are particularly active in the domesticated cells. Therefore, a series of mutations occurred in the regulatory factors, such as transcription factors and translation initiation factors. For example, genes in PF00806 create protein gradients by regulating translation and mRNA stability causing asymmetric cell division and regulating cell fate specification [6].

However, some functions showed significant down-regulation due to reliable mutation, including some associated with respiration. PF07992 and PF02852 were both down-regulated. These are mainly domains inside class I and class II oxidoreductases, as well as NADH oxidases and peroxidases [72,74]. Additionally, PF07992 represents small NADH binding domains within a larger FAD binding domain [65,73]. The genetic mutations and transcriptional changes observed for these two protein families further support the speculative conclusion, as presented in section 3.1, that either NADP or NAD is promoted while FAD must be inhibited. As for the competition between NADP and NAD, the NADP process is more likely to be promoted than the NAD process. This result may be an extension of the competition between the genes involved in the light response mentioned before. Specifically, chlorophyll synthesis, which provides the basis for photosynthesis, outcompetes cytochrome *c* synthesis, which provides the basis for respiration. As a result, the respiratory electron transport chain was slightly degraded to accommodate a cellular environment in which photosynthesis overtakes respiration. Therefore, oxidative phosphorylation was inhibited in the domesticated strains. It is conceivable that in the domesticated microalgae, the main pathway providing a sufficient ATP supply changed from oxidative phosphorylation to photophosphorylation and substrate-level phosphorylation [33]. The alternative is proteolysis. For instance, the down-regulated protein family PF00240 known as ubiquitin acts via ubiquitinylation of other proteins, which are then targeted for destruction by the 26S proteasome [5]. Because proteolysis destroys proteins, up-regulation of proteolytic enzyme expression is beneficial to destroy cells [52]. Although the significance of proteolysis in microalgal cells has not been thoroughly studied, it is conceivable that the more stable internal environment of the domesticated cells can lead to a significant decrease in the demand for proteolytic enzymes and a corresponding degradation of proteolytic function.

In summary, CO_2 gradient acclimation not only caused multiple targeted mutations, but also showed strong functional preference. This resulted in the natural mutation and selection, as induced by CO_2 gradient domestication, exhibiting certain characteristics of directed mutation, but with more extensive active sites in the genome. In the domesticated strains, enzymes for light response, especially those related to chlorophyll synthesis, became the center of the gene mutating system with corresponding improvements in carbohydrate metabolism, cytogenesis and some transporters, as well as inhibition of respiration and proteolysis. These made up the basic features at the genetic level of the domesticated strains subjected to CO_2 gradient acclimation.

3.3. Functional enrichment of differentially expressed genes developed by gene mutation and natural selection in CO_2 gradient acclimation

Multiple targeted mutations caused by CO_2 gradient domestication resulted in universal changes at the transcriptomic level in the domesticated strains. From the whole transcriptome perspective, the GO and PF functions that exhibited significant changes in expression are listed in Fig. 4(a) and (b), respectively. As shown in Fig. 4(a), when considering the broad functional category for GO entries that exhibited significant expression changes, the up-regulated categories with>3 entries consisted of cytogenesis, metabolism of energy storage substances, transport and catalysis (for respiration or photosynthesis, mainly related to coenzymes). In addition, the only down-regulated category with>3 entries was proteolysis.

In the broad category of cytogenesis, GO entries with significant up-regulation (note: a large number of duplicated entries involving identical genes were removed from the analysis) included those categorized as small GTPase binding, nucleobase-containing small molecule, molecule biosynthetic process, RNA methyltransferase activity, nucleotide phosphorylation, mRNA metabolic process, tetrapyrrole metabolic process, ribose phosphate metabolic process, ribonucleotide biosynthetic process, tetrapyrrole biosynthetic process, DNA-directed 5′-3′ RNA polymerase activity, DNA polymerase activity, organophosphate biosynthetic process, transferase complex, transferring, phosphorus-containing groups and unfolded protein binding. It was observed that the whole system related to genetic material synthesis, transcriptional processes and even protein synthesis were fully promoted in the domesticated strains. Moreover, in the broad category of metabolism of energy storage substances, GO entries with significant up-regulation included those categorized as glycerolipid biosynthetic process/lipopolysaccharide metabolic process; glycolytic process; aromatic compound catabolic process; transferase activity; transferring alkyl or aryl (other than methyl) groups; cellular carbohydrate metabolic process; carbohydrate derivative biosynthetic process; phospholipid metabolic process; and carbohydrate derivative metabolic process. The whole system related to carbohydrate metabolism was boosted. In addition, the broad category of catalysis included three GO entries: coenzyme biosynthetic process, coenzyme metabolic process and cofactor biosynthetic process. Combined with the analyses in sections 3.1 and 3.2, the benefits of the promoted coenzyme processes could primarily aid in photosynthetic electron transfer. Nevertheless, the enhanced coenzyme processes were beneficial to the physiological and metabolic processes in the domesticated cells. In contrast, the most dominant broad category exhibiting universal down-regulation was proteolysis, and included GO entries categorized as cellular protein catabolic process, peptidase complex, protein modification by small protein conjugation and modification-

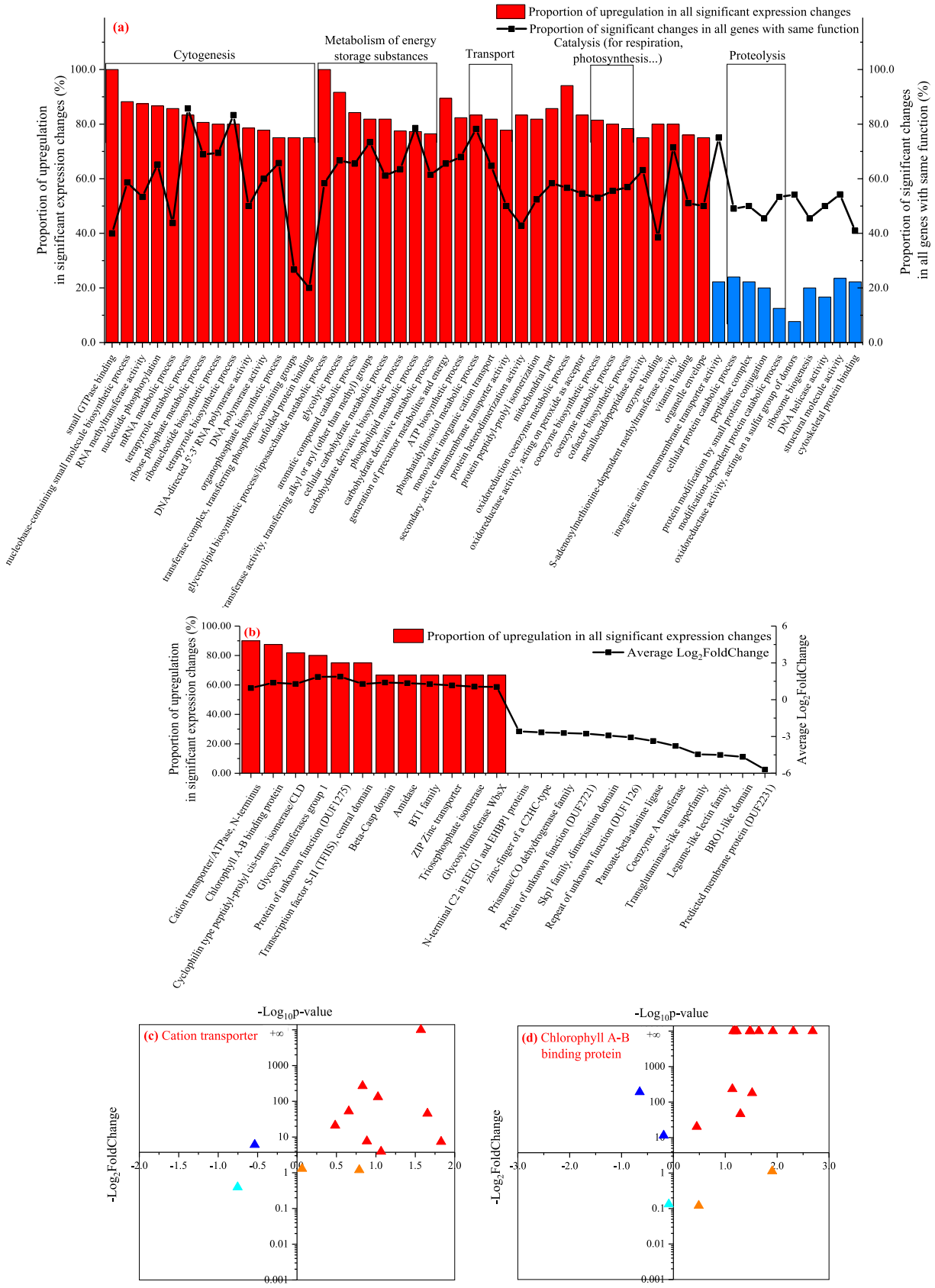

Fig. 4. Significant up-regulation/down-regulation of transcriptome expression. (a) GO category, (b) PF family, expression changes of all genes in the family of (c) cation transporter and (d) chlorophyll *A*-B binding proteins (using red represents the up-regulation and blue represents the down-regulation, shallow orange and shallow blue represent the gene with insignificant changes).

dependent protein catabolic process. These phenomena, observed at the whole transcriptional level, were consistent with the function of previous gene mutations and were also directly related to transcriptional differences.

According to the rank based on the proportion of up-regulated genes of those with a significant change in transcriptomic level, the three most significantly up-regulated PF entries all included>10 genes with expressional changes, namely cation transporter/ATPase (N-terminus), chlorophyll *A*-B binding protein and cyclophilin type peptidyl-prolyl cis–trans isomerase/CLD (Fig. 4(b)). The cation transporter/ATPase (N-terminus) PF00690 family includes transmembrane ATPases for ions, such as exchange P-ATPases of H^+, Na^+, Ca^{2+}, Na^+/K^+ and H^+/K^+. Because transmembrane ion transport plays an important role in the intracellular pH balance under high CO_2 concentrations [41], the improvement of P-ATPases may effectively enhance tolerance to CO_2. Furthermore, the universal up-regulation of chlorophyll *A*-B binding protein (PF00504) is directly implicated in the increased light-harvesting antenna, which catches light quantum during photosynthesis, providing an effective material basis for the active light reaction [46]. The expression of genes within these two protein families are shown in Fig. 4(c) and (d), in which most genes represent a significant up-regulation in expression with FDR < 0.05. These two results were consistent with the functional analysis of gene mutations, especially with respect to the increase of light-harvesting chlorophyll *A*-B binding proteins, which may be the direct result of the enhanced chlorophyll synthesis pathway due to mutation of magnesium chelatase (EC 6.6.1.1). Additionally, the mutations of positive significance in other light response proteins may also take part in the Chl binding to light-harvesting proteins, similar to the role of some light-inducible proteins (LIL_1, LIL_3) [58]. Expressional changes in these two protein families laid an effective foundation for enhancing photosynthesis and CO_2 tolerance. In addition, the proteins in the cyclophilin-type peptidyl-prolyl cis–trans isomerase/CLD (PF00160) family represented an important series of regulator cyclophilins with peptidyl-prolyl cis–trans isomerase (EC 5.2.1.8). Some members have been demonstrated as responsible for protein folding processes and enabling transcriptional events [59]. Thus, the up-regulation of this protein family may improve transcription and protein synthesis for cell construction. From the prospective of transcription, the processes of light response, transport and cytogenesis were still primarily enhanced in the domesticated cells during CO_2 gradient acclimation.

3.4. Improvement in photosynthetic light reaction through CO_2 gradient acclimation

The core of CO_2 tolerance is the photosynthetic carbon fixation system of microalgae. As the electron support for the Calvin cycle of CO_2 fixation, the light reaction partly decides the strength of photosynthesis. According to the genetic and transcriptomic analyses, enzymes related to the light reaction became the focus of natural mutation and selection in microalgae during the CO_2 gradient acclimation. It can be assumed that huge differences appeared in the light reaction, subsequently initiating characteristic changes in the photosynthetic carbon fixation system. A series of tests on the photosynthetic light reactions were carried out to determine the effect of the CO_2 gradient during different stages of *N. oceanica* CCMP1779 acclimation (Fig. 5).

Above all, the rapid light curves showed that electron transport for photosynthesis was gradually enhanced from AD, 6D to 12D (Fig. 5(a) and (b)). Compared to AD, the rETRmax of 12D increased by 211.2% during gradient acclimation. After exposure to 15% CO_2, the rETRmax of 12D decreased but was still 85.5% higher than AD and 12.3% higher than 6D under the same conditions, respectively. A similar phenomenon was observed for I_k and α. These parameters demonstrate that CO_2 gradient acclimation gradually enhances the electron transfer process of *N. oceanica* CCMP1779 for photochemistry, and that the amount of light quantum that microalgal cells can capture and utilize gradually increases. High CO_2 exerted a common inhibitory effect for photochemical systems of AD, 6D and 12D, but 12D still showed the strongest resistance to CO_2 stress. Thus, its photochemical electron transfer performance was still the best under 15% CO_2 conditions. This may be a direct result of the overall increase in light harvesting protein expression, enhancement of cation transport and promotion of free Mg^{2+} for stacking of photosynthetic chloroplast membranes.

With fast saturation pulses, 12D showed the most sensitive recovery of the photosynthetic electron transport chain through the largest drop of photosynthetic fluorescence (F_{PS}) after the extinguishment of the saturation pulse (Fig. 5(c) and (d)). Additionally, the secondary peak (ΦS) caused by the rapidly applied secondary saturation pulse first increased and then decreased during the domestication process. In the two12D groups, this secondary peak decreased to almost 0. The rise from AD to 6D may indicate that transient light protection mechanisms, such as sensitively shutting down photosynthetic reaction centers, were first enhanced during domestication. However, the sharp drop from 6D to 12D may cause the microalgal strains to procure the transient ability to adjust the light reaction system to enable stable operation of the electron transport chain mechanism. Examples of this include the rapid response of PSI or transformation of the light harvesting protein from PSII to PSI, which enhanced PSI in the downstream electron transport chain during the moment of the second pulse. Thus, the secondary peak caused by the second pulse almost disappeared. In this measurement, both ΦPS and ΦS of AD under 15% CO_2 were abnormally high. This was mainly because the fluorescent peak of AD under 15% CO_2 (Fm) was too low when the first saturation pulse was received. In other words, the Fv/Fm of AD under 15% CO_2 was too low (only ~ 0.6), indicating that under 15% CO_2, the whole light reaction system is comprehensively suppressed or even destroyed (Fig. 5(c)).

When considering the light protection ability of AD, 6D and 12D (Fig. 5(e) and (f)), the total volume of non-photochemical quenching showed a slight decrease of 22.7% from AD to 12D with actinic light (1200 μmol/(m^2·s)), mainly because of the significant decrease of the slow NPQ phase by 67.7%. A similar decrease of the slow phase also appeared with actinic light at 800 μmol/(m^2·s), but the absolute values of the slow phase were lower than those with 1200 μmol/(m^2·s). This result demonstrates that CO_2 gradient acclimation enables microalgae to gain a more flexible NPQ method because slow phase components that inhibit the rapid recovery of normal electron transfer gradually declined. Additionally, the NPQ of AD under 15% CO_2 with 1200 μmol/(m^2·s) actinic light appeared to have an abnormal decline, which may represent the destruction of the AD light protection system after transferring to the high CO_2 condition.

In addition, according to the slope of post-illumination curves, after gradual domestication the PSI intensity effectively increased under 15% CO_2 (Fig. 5(g) and (h)). From AD to 6D, the PSI intensity increased by 1.67-fold, while it increased by 2.65-fold from AD to 12D. Enhancement of the PSI indicates that the acclimated algal species possessed more unobstructed cyclic electron transfer under the adverse high CO_2 condition, which promoted photosynthesis and ATP synthesis in the chloroplast.

3.5. Improvement of the photosynthetic dark reaction through CO_2 gradient acclimation

According to the expression of key enzymes related to inorganic carbon transport and CO_2 fixation (Fig. 6 and Supplementary File 4), a changing tendency due to CO_2 gradient acclimation could be summarized into three parts: improved inorganic carbon transport, a more powerful C4 mechanism for CO_2 storage and an enhanced Calvin Cycle. The first group of genes, known as Ci–regulated genes [12], which include *CAH-1*, *CAH-2*, *CCP* and *LCIA* were found in *N. oceanica* CCMP1779 and are involved in transmembrane inorganic carbon transport. Based on the results of the RT-qPCR, the transcription of *CCP* and *LCIA* was enhanced from AD to 12D during the process of CO_2

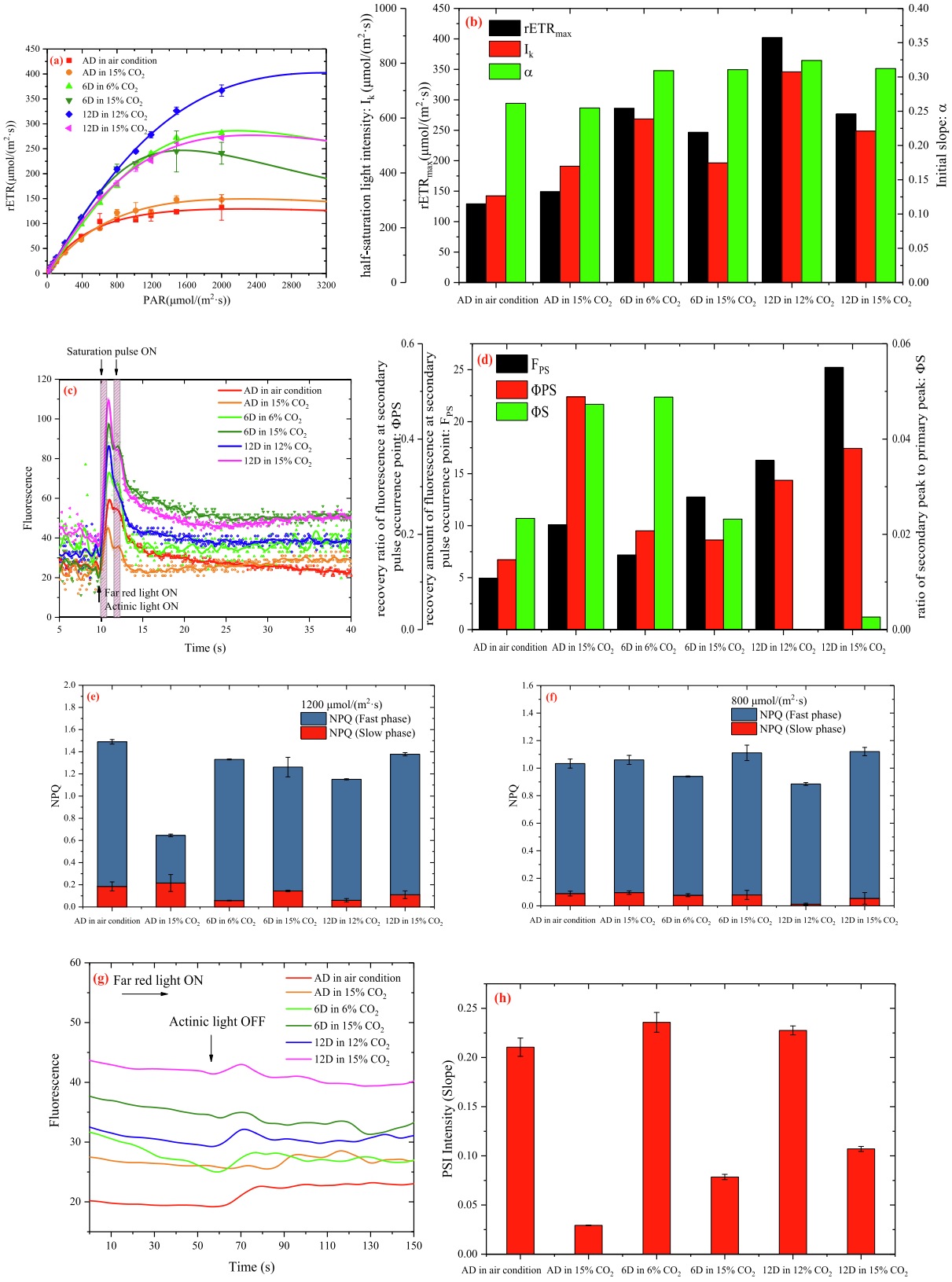

Fig. 5. Changes of photosynthetic parameters in microalgae strains gradually domesticated with 6% and 12% CO_2 and then cultivated with 6 mL/min 15% CO_2. (a) Rapid light curves, (b) maximum relative photosynthetic electron transfer rate ($rETR_{max}$), half-saturation light intensity (I_k) and initial slope (α) of rapid light curves, (c) continuous saturation pulse response, (d) recovery amount of fluorescence at secondary pulse occurrence point (F_{PS}), recovery ratio of fluorescence at secondary pulse occurrence point (ΦPS) and ratio of secondary peak to primary peak (ΦS), Non photochemical quenching at (e) 1200 μmol/(m^2·s) and (f) 800 μmol/(m^2·s), (g) post-illumination curves and (h) slopes to reflect PSI intensity.

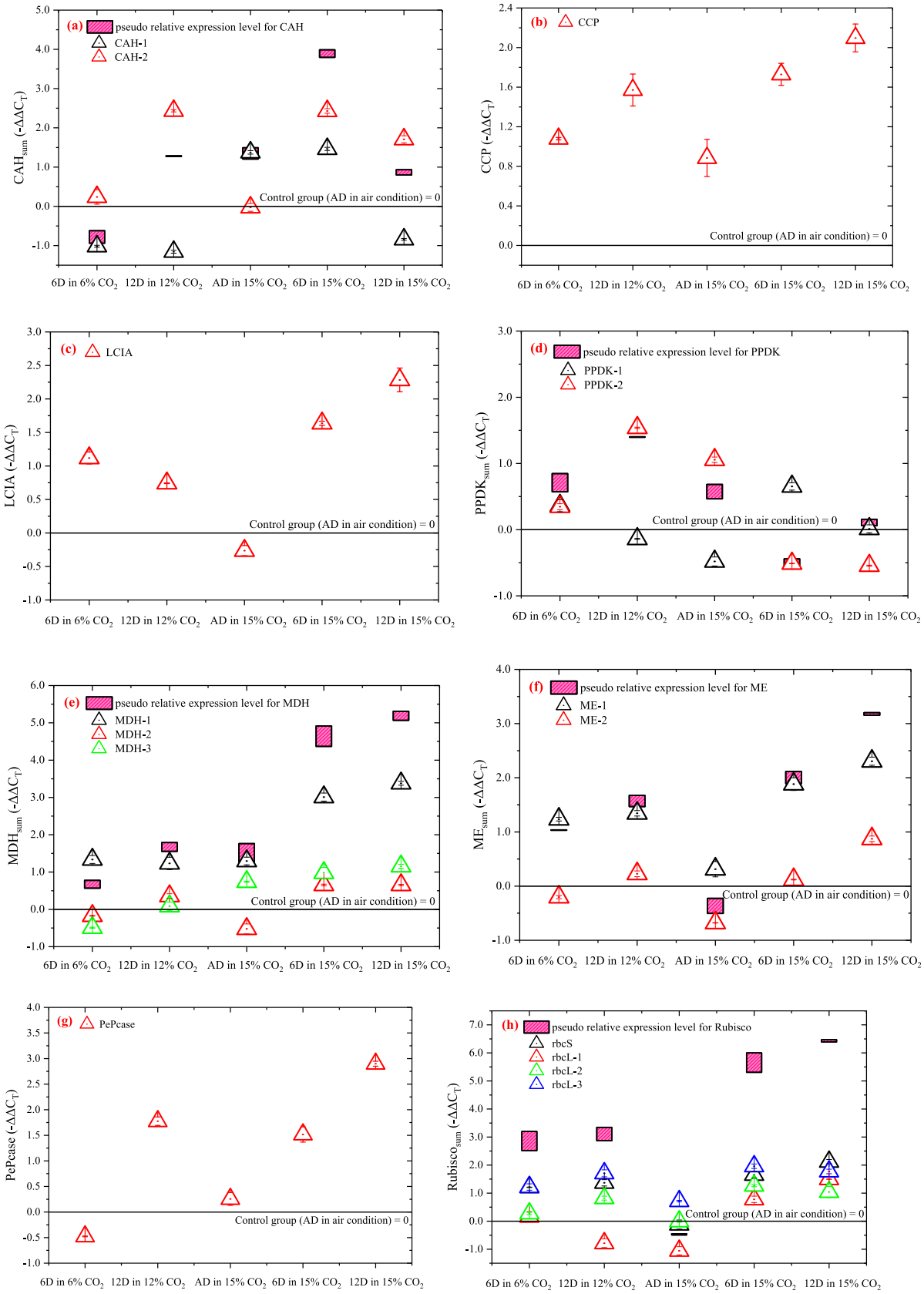

Fig. 6. RT-PCR for key enzymes on CO_2 transport and photosynthetic dark reaction in microalgae strains gradually domesticated with 6% and 12% CO_2 and then cultivated with 6 mL/min 15% CO_2. These enzymes consist of (a) carbonic anhydrase, transmembrane transport enzymes for inorganic carbon (b) CCP and (c) LCIA, (d) pyruvate, phosphate dikinase, (e) malate dehydrogenase, (f) malic enzyme, (g) phosphenolpyruvate carboxylase and (h) RuBisCO.

gradient acclimation. After transferring to 15% CO_2, their transcription in the domesticated strains was further enhanced with -$\Delta\Delta C_t$ up to>2.0 while wild-type AD maintained a low expressional level (Fig. 6(b) and (c)). However, the carbonic anhydrases *CAH-1* and *CAH-2*, responsible for the conversion of CO_2 and HCO_3^-, represented a complex changing tendency. *CAH-1* always maintained a very low expressional level in the domesticated strain (12D), but it was increased in undomesticated and insufficiently domesticated strains (AD and 6D) after exposure to 15% CO_2. On the contrary, the expression of *CAH-2* was much higher in 6D and 12D when compared with wild-type AD, both during the process of CO_2 gradient acclimation and under 15% CO_2 (Fig. 6(a)). In other words, the transcription of carbonic anhydrase isoenzymes in *N. oceanica* CCMP1779 appeared to be very diverse, which may lead to some differences in metabolism.

At least nine carbonic anhydrases have been identified *Chlamydomonas reinhardtii* and they are distributed in different intracellular spaces [81]. Among them, only *CAH3*, located inside the pyrenoid, is responsible for the final step of converting HCO_3^- to CO_2 for directly providing CO_2 to RuBisCO, while carbonic anhydrases located in other subcellular structures are more important for regulating the intracellular balance of ions and pH through the conversion of CO_2 and HCO_3^- [42]. Two carbonic anhydrase encoding genes (*CAH-1* and *CAH-2*) have been previously identified in *N. oceanica* CCMP1779 [3]. *CAH-1* has been located in the lumen of the epiplastid ER and plays an important role in concentrating inorganic carbon in low CO_2 environments [10]. Therefore, its down-regulation in the fully domesticated strain may inhibit excessive conversion of CO_2 to HCO_3^- to release too much H^+, thereby destroying the intracellular pH balance. When undomesticated and insufficiently domesticated strains moved to 15% CO_2, the sudden increase of *CAH-1* expression could lead to the excessive accumulation of H^+ inside the cell, which would cause a negative effect on survive under high CO_2 concentrations. This false stress response reflects the disorder of internal regulation for insufficiently domesticated strains after transplantation to high CO_2. In the 6D stain with a relatively higher active carbon fixation mechanism, even the increase of *CAH-1* was slightly more dramatic. However, gradual domestication could effectively solve this problem.

The biggest problem was related to *CAH-2*, the location and function of which have not been studied in previous literature. Only one previous study conjectured that *CAH-2* may likely be implicated in regulation of the CO_2 concentration mechanism (CCM) in response to variation of CO_2 concentration [48], but further evidence and analysis is still lacking. It could be that *CAH-2* may act as an inhibitor of the whole CCM process to prevent too much conversion from CO_2 to HCO_3^- in response to a high concentration of CO_2. Therefore, with a sufficient CO_2 supply (which would never cause inhibition to wild-type), *CAH-2* knockdown strains grow even faster than wild-type *N. oceanica* CCMP1779, but they showed no difference in growth under the air condition [48]. Thus, in this research, the overexpression of *CAH-2* may have inhibited the active transport of HCO_3^-, one of the major modes of intracellular CO_2 transmission in *N. oceanica*, by reducing the generation of HCO_3^-, but it also improved the survival rate of the microalgae under high CO_2 by stabilizing the pH. However, there was no doubt that the transmembrane transport HCO_3^- module, composed of *CCP* and *LCIA*, was effectively improved in the domesticated strains. This enabled the limited HCO_3^- to rapidly concentrate to RuBisCO in the chloroplast, thereby accelerating the carbon fixation efficiency [44,54].

Key enzymes, except for phosphate dikinases (*PPDK*), in the C4 pathway, which is another pathway for HCO_3^- to concentrate for RuBisCO and the Calvin Cycle, were all substantially up-regulated in the strains domesticated with a CO_2 gradient, which were increased further after transferring to 15% CO_2. Conversely, wild-type AD always showed low expressional level for those enzymes (Fig. 6(e)-(g)). The expression of *PPDK*, the rate-limiting enzyme in C4 mechanism [76], decreased in the domesticated strains when high carbon stress with 15% CO_2 replaced the original cultivation environment (Fig. 6(d)). Since the C4 pathway temporarily locks exogenous CO_2 or HCO_3^- into malate, there are two possible divergent pathways. The first is the conversion of malate into oxaloacetate through a reversible malate dehydrogenase-guided catalytic reaction. The second pathway, catalyzed by the malic enzyme and the rate-limiting enzyme *PPDK*, releases CO_2 and returns to the beginning of the C4 cycle. Thus, in combination with the increased expression of a series of malate dehydrogenases in the domesticated strains (Fig. 6(e)), the decreased *PPDK* expression indicates that the C4 pathway led to a stronger inner cycle of C element from CO_2 as the C4 intermediates (such as malate and oxaloacetate). After CO_2 gradient acclimation, the C4 pathway was enhanced, so more inorganic carbon was catalyzed into this pathway. However, the completion rate of the C4 cycle, which releases CO_2 to the RuBisCO enzyme, became slower in the domesticated strains. Therefore, in a high carbon environment, the domesticated strains strongly activated the C4 pathway not to concentrate carbon for improving the photosynthetic CO_2 fixation rate with Calvin Cycle, but to allow inorganic carbon to exist in a wider range of inorganic carbon forms, thereby storing more CO_2 with limited RuBisCO to release during high CO_2 stress. The enhancement of C4 pathway by high CO_2 concentration may provide multiple carbon fixation pathways to C3 microalgae and finally improve their CO_2 fixation ability [14]. Although some articles believed that overexpressing C4 genes in C3 plants cannot significantly improve the photosynthetic capacity of the plants [80], but at least it improved the stress resistance [49]. One possible mechanism for this is the up-regulation of *PePcase* induced by the enhancement of the regulatory pathway of intracellular pH homeostasis; thus improving the ability to resist acidification brought by CO_2 due to accumulation of the buffer material oxaloacetate and L-malate [76].

At last, as the core of the carbon fixation system in *N. oceanica*, RuBisCO mainly determines the CO_2 fixation ability. In this research, the expression of genes related to RuBisCO (*rbcS*, *rbcL-1*, *rbcL-2* and *rbcL-3*) all showed the same tendency in strains with different acclimation stages. Specifically, they were gradually up-regulated from strains AD to 12D during the process of CO_2 gradient acclimation. Moreover, after transferring to 15% CO_2, the expression was up-regulated further in the domesticated strains while it did not change significantly in AD (Fig. 6 (h)). This demonstrates that domesticated strains would have a more effective dark reaction for CO_2 fixation when facing high CO_2 stress, whereas it was difficult for wild-type AD to mount an effective response to high CO_2 stress via self-regulation.

3.6. Enhanced biomass productivity and CO_2 tolerance by CO_2 gradient acclimation against high CO_2 concentration

In this research, two cultivation tests with 15% CO_2 gas were carried out to investigate the improvement stimulated by the CO_2 gradient acclimation process on microalgae. Actual flue gas from the coal industry often has a 15% CO_2, but this concentration has been shown to inhibit the growth of *N. oceanica* [67]. For the first experiment, with a 12 mL/min aeration rate of stimulated flue gas, the biomass yield after 8 days cultivation of microalgal strains obtained after different stages of CO_2 gradient domestication was determined (Fig. 7(a)). The wild-type AD strain could not survive and grow in 12 mL/min 15% CO_2. Its biomass yield decreased by 16.3% from day 0 to day 8 because of cell death and decomposition. Similarly, the biomass yield of strains 3D and 6D could not tolerate the 12 mL/min 15% CO_2, although their biomass yields were slightly higher than AD. For strains AD, 3D and 6D, due to their failure to absorb inorganic carbon and regulate ion balance, the pH declined from day 1 after which the extracellular pH dropped below 6.0 and became increasingly close to 5.6 (pH of carbonic acid) (Fig. 7(b)). At the same time, the proportion of surviving cells from these three strains decreased to around 10% at day 6 (Fig. 7(c)), which demonstrates that the negative effect of high CO_2 stress not only causes growth cessation but also induces mass cell death. Therefore, it was impossible for the undomesticated and insufficiently domesticated microalgal strains to

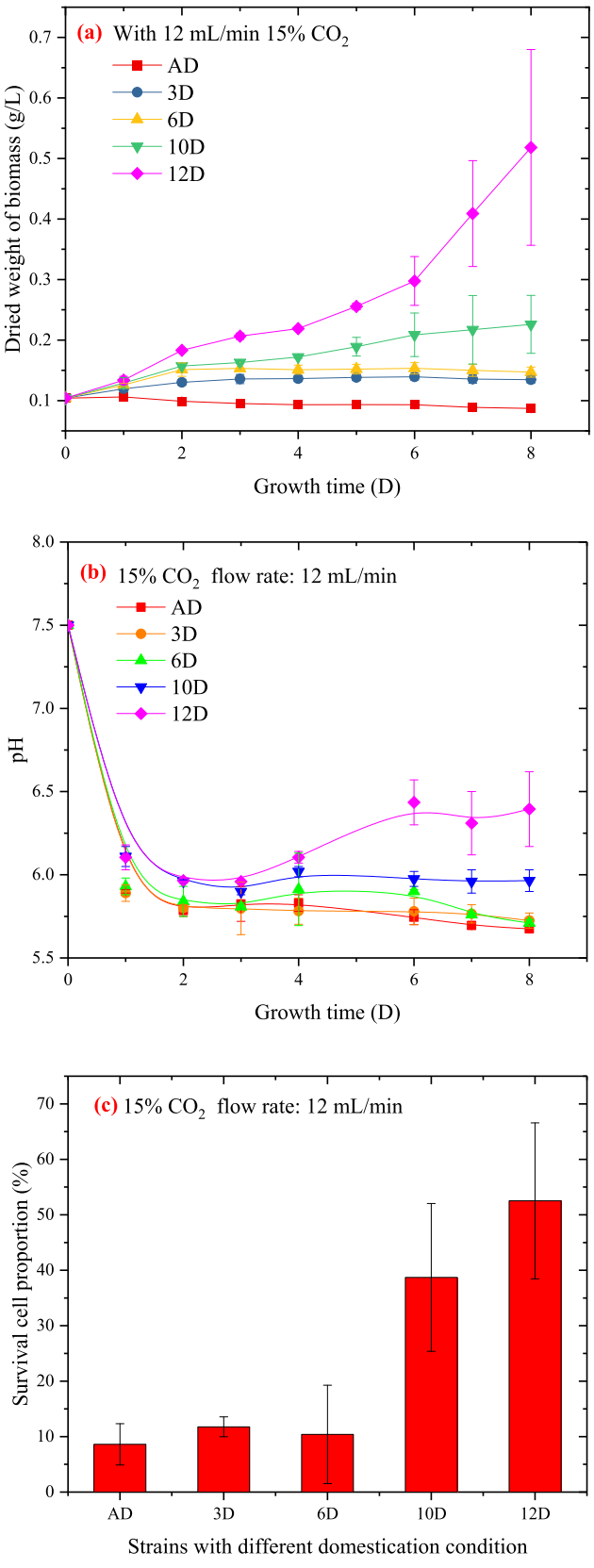

Fig. 7. Growth performance of *N. oceanica* strains (gradually domesticated with various concentrations of CO_2) cultivated with 12 mL/min 15% CO_2. (a) Biomass, (b) pH and (c) survival cell proportion.

adapt to the high CO_2 concentration without any self-adjusting. However, 10D, with further gradient acclimation, showed a possibility to survive in 12 mL/min 15% CO_2. Compared to day 0, the biomass yield increased by 117.7% on day 8. When the domestication stage proceeded to 12% CO_2, the obtained 12D strain showed a predominant survive ability at an extremely high CO_2 concentration for a wild-type strain. The biomass yield on day 8 was 3.98-fold higher than that on day 0. As a result of the strong inorganic carbon fixation and transmembrane ion transport abilities, the extracellular pH returned to 6.4 (Fig. 7(b)), and the proportion of surviving cells remained 52.5% on day 6 (Fig. 7(c)). This shows the possibility that the fully domesticated 12D strain could continue to grow at extremely high CO_2 concentrations.

When the CO_2 concentration was more moderate at an aeration flow of 6 mL/min, the microalgal strains after CO_2 gradient acclimation still showed superior growth features when compared to the wild-type (Fig. 8(a)). From day 0 to day 8, the biomass yield of AD only increased by 25.3% with a very slow rate, while the biomass of 3D, 6D and 10D increased 20-fold, with the most predominant increase in biomass yield (22.7-fold) for 12D. The domesticated strains all continued to grow, so the changing tendency of pH in those four groups did not show large differences with a final extracellular pH of around 6.8, while the extracellular pH of the AD group could not return to 6.0 (Fig. 8(b)). However, the extracellular pH of 12D recovered faster than the other groups (on day 2, the pH of 12D was 6.8 while other groups were still below 6.5). This shows that under a high CO_2 concentration, the logarithmic growth and photosynthetic carbon sequestration processes of 12D were restored faster to better adapt to high CO_2 than those of the other insufficiently domesticated strains. As further evidence, the chlorophyll and carotenoid contents of 12D were almost double that of the other three groups of insufficiently domesticated strains before day 4, while AD could not normally synthesize photosynthetic pigments during the whole cultivation period (Fig. 8(c) and (d)). Therefore, it can be expected that in large-scale industrial microalgal cultivation with a shorter culture period (around 2–4 days), CO_2 gradient acclimation will provide microalgae with better growth characteristics and higher CO_2 tolerance.

Compared with other studies in recent years (Table 1), the *N. oceanica* strains obtained in this study achieved good tolerance to high CO_2 flow rate, showing the highest biomass yield and growth rate with $>$ 0.001 vvm CO_2 flow rate (CO_2 gas proportion $>$ 2%). Although the CO_2 tolerance and growth rate would also be affected by other conditions, such as the specific microalgal strain, different photoreactors and light intensity, it also could be seen that the gradual domestication method used in this experiment obtained a relatively ideal CO_2 tolerance ability.

4. Discussion

There have been many attempts to gradually domesticate microalgae to improve growth characteristics and achieved some satisfactory results with different microalgal species [1,11,13,19,28,30]. If successful, this method may confer the advantages of simple operation, high success rate, large scale operation and more adaptability for industrial microalgal cultivation. Cultivation of *N. oceanica* through this method achieved the ideal characteristics of a fast growth rate and high tolerance to high CO_2 stress. Furthermore, the gradual changes in *N. oceanica* CCMP1779 during the CO_2 gradient acclimation were clarified to show the significance on obtaining strain tolerance to high CO_2 in flue gas.

Multi-targeted gene mutations appeared in the domesticated strains, demonstrating that CO_2 gradient acclimation requires the natural mutation and screening of strains, instead of a temporary adaption to environment. CO_2 gradient acclimation for high CO_2 adaptation was particularly suitable to induce targeted group evolution because microalgae can multiply rapidly over many generations in a very short time under a carbon-rich environment. Thus, conditions were provided for sufficient gene mutation, and traits suitable for this environment

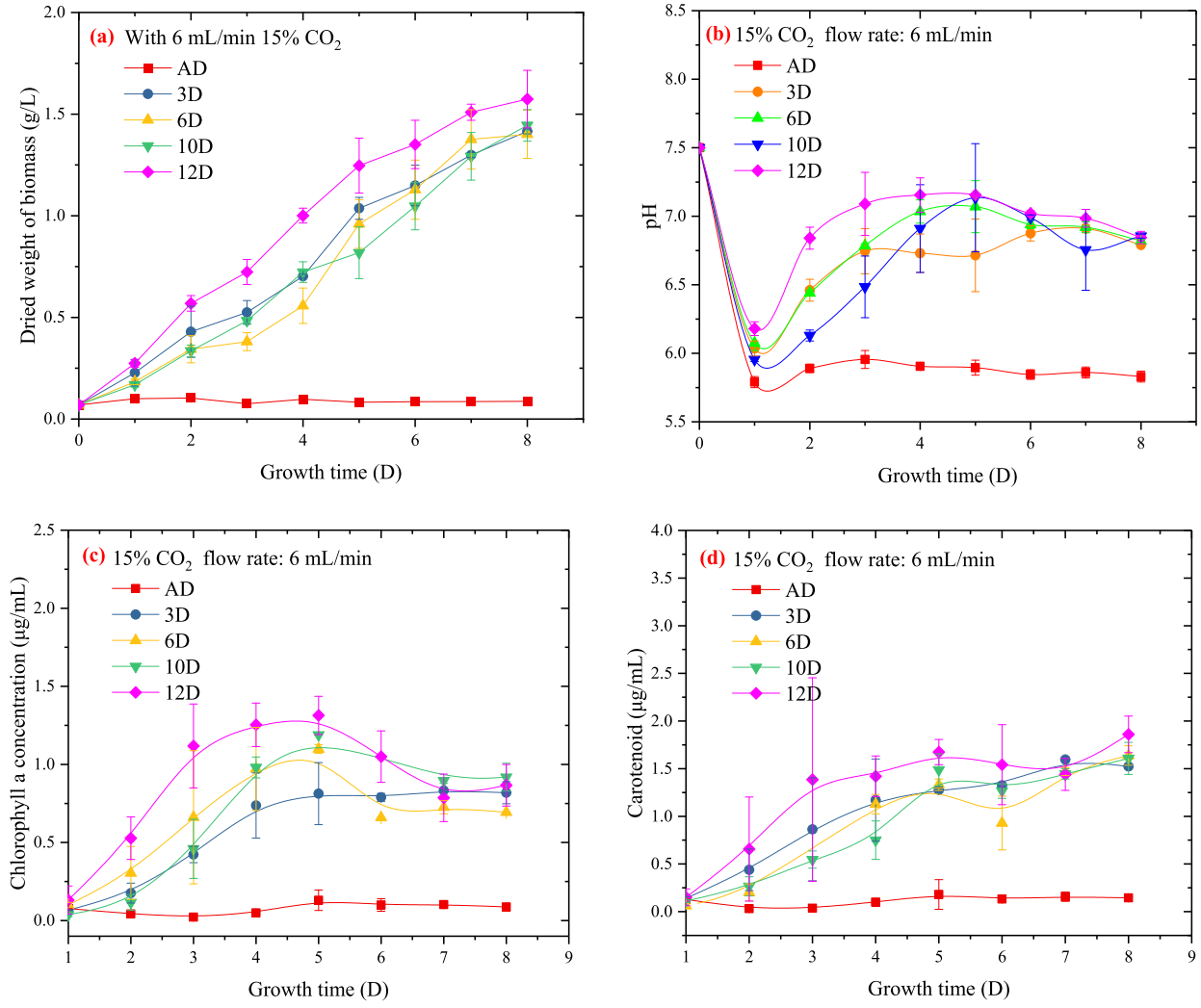

Fig. 8. Growth performance of *N. oceanica* strains (gradually domesticated with various concentrations of CO_2) cultivated with 6 mL/min 15% CO_2. (a) Biomass, (b) pH, (c) chlorophyll *a* concentration and (d) carotenoid concentration.

Table 1
Comparison of tolerance of *N. oceanica* to high CO_2 in recent studies. (Notes: Mainly list the maximum CO_2 concentration conditions used in literatures, or the CO_2 supply conditions close to that of this research).

CO_2 proportion in gas (%)	Gas flow rate (vvm)	**CO_2 flow rate (vvm)**	**Final biomass yield (g/L)**	Original biomass yield before cultivation (g/L)	**Average growth rate (g/L/d)**	Researchers
15%	0.04	**0.006**	**0.52**	0.1	**0.053**	This article
15%	0.02	**0.003**	**1.6**	0.1	**0.188**	
20%	0.029	**0.0058**	**0.6**	0.2	**0.0417**	Lestari et al.[63]
15%	0.007	**0.00105**	**Complete suppression (No increase in biomass)**			Zhang et al.[38]
5%	unclear	**unclear**	**1.55**	~0.1	**0.145**	Li et al.[47]
2%	unclear	**unclear**	**0.87**	unclear	**~0.087**	Vikramathithan et al.[37]
15%	0.015	**0.00225**	**1.4**	0.1	**0.186**	Zhu et al.[82]
5%	changing to keep pH = 8–8.3	**unclear**	**unclear**	unclear	**0.13**	Pedersen et al.[75]
15%	0.05 (24 h average)	**0.0075**	**0.56**	0.03	**0.038**	Wang et al.[70]
6%	0.5	**0.03**	**0.27**	0.03	**0.0256**	Chen et al.[78]

could be easily enriched in the population so that multiple sets of reliable mutations were present from "aa" (reference genome genotype) to "AA" (mutant genotype), from recessive homozygous to dominant homozygous. In addition, multiple-stage CO_2 gradient acclimation enabled the microalgae to gradually approach the targeted stress environment. During acclimation, natural selection was more likely to occur due to the overwhelming adaptation of microalgal cells with favorable traits. The high survival rate of microalgae was always maintained, which improves the reliability and success rate of this method.

Observation of photosynthesis and growth under high-carbon conditions showed that sufficient domestication was far better than insufficient domestication. As the end point of the acclimation stage became

closer to the target stress condition, the domesticated microalgal strains better exhibited the desired light reaction performance, expression of dark reactive enzymes and photosynthetic characteristics after altering the target stress condition. Sometimes the little difference was a matter of success or failure. For example, under 12 mL/min 15% CO_2, the insufficiently domesticated 6D could not survive, but 12D still showed strong growth potential. This may be due to large differences in the expression response of carbonic anhydrase and the photosynthetic electron transport capacity. During further domestication, key intracellular physiological processes would modulate to a level more adaptable to targeted stress conditions.

Different from the low CO_2 in different atmospheric conditions, the high concentration of CO_2 in flue gas is able to enter the cell via two mechanisms: 1) diffusion and mass transfer of the CO_2 molecule across the membrane occurs due to the pressure gradient difference of extracellular and intracellular CO_2; and 2) extracellular CO_2 dissolves in the liquid microalgal cultivation medium, releasing H^+ and HCO_3^-, and thus HCO_3^- is transported into the cell by ion active transport. The latter mechanism has been more widely discussed because under natural atmospheric conditions, cells generally rely on the CCM mechanism to condense and transport dissolved HCO_3^- to provide carbon for photosynthesis. However, in the flue gas environment, a large and continuous pressure gradient of CO_2 inevitably makes the direct diffusion of CO_2 the main pathway for inorganic carbon accumulation, thereby allowing large amounts of CO_2 to accumulate inside the cell. Therefore, the entire photosynthetic system does not lack CO_2, and even the CO_2 consumption rate of the whole photosynthetic system cannot catch up with the CO_2 accumulation rate in the cells, thus leading to a persistent surplus of CO_2. In this case, excess and unconsumable intracellular CO_2 leads to a series of negative consequences. Perhaps most crucially, CO_2 must follow chemical rules for dissolving and ionizing into H^+ and HCO_3^- in the intracellular solute. Accordingly, the presence of intracellular carbonic anhydrase will greatly accelerate this process. Thus, excess H^+ reduces the intracellular pH, inhibits growth, and even destroys cells. Surely, H^+ can be transported out of the cell through multiple ion channels, but without exception, this transport requires ATP consumption, and when the rate of ATP synthesis fails to keep up with the ion transport requirements, cell destruction becomes inevitable.

At present, genetic engineering of microalgal strains to adapt to high CO_2 environments is basically centered on knocking down carbonic anhydrase. This destroys the intracellular transformation system between CO_2 and HCO_3^- by reducing the speed of conversion between the two, which protects the intracellular pH homeostasis and reduces apoptosis. This scheme has achieved remarkable results[47]; however, byobserving CO_2 gradient acclimation of *N. oceanica* CCMP1779, another mechanism in which microalgae self-regulate to adapt to a high carbon environment is clearly possible (Fig. 9). It is comprehensible that improving photosynthesis is the key to truly addressing the negative consequences of high CO_2 and making full use of carbon sources to increase biomass production under high CO_2 conditions. Therefore, this

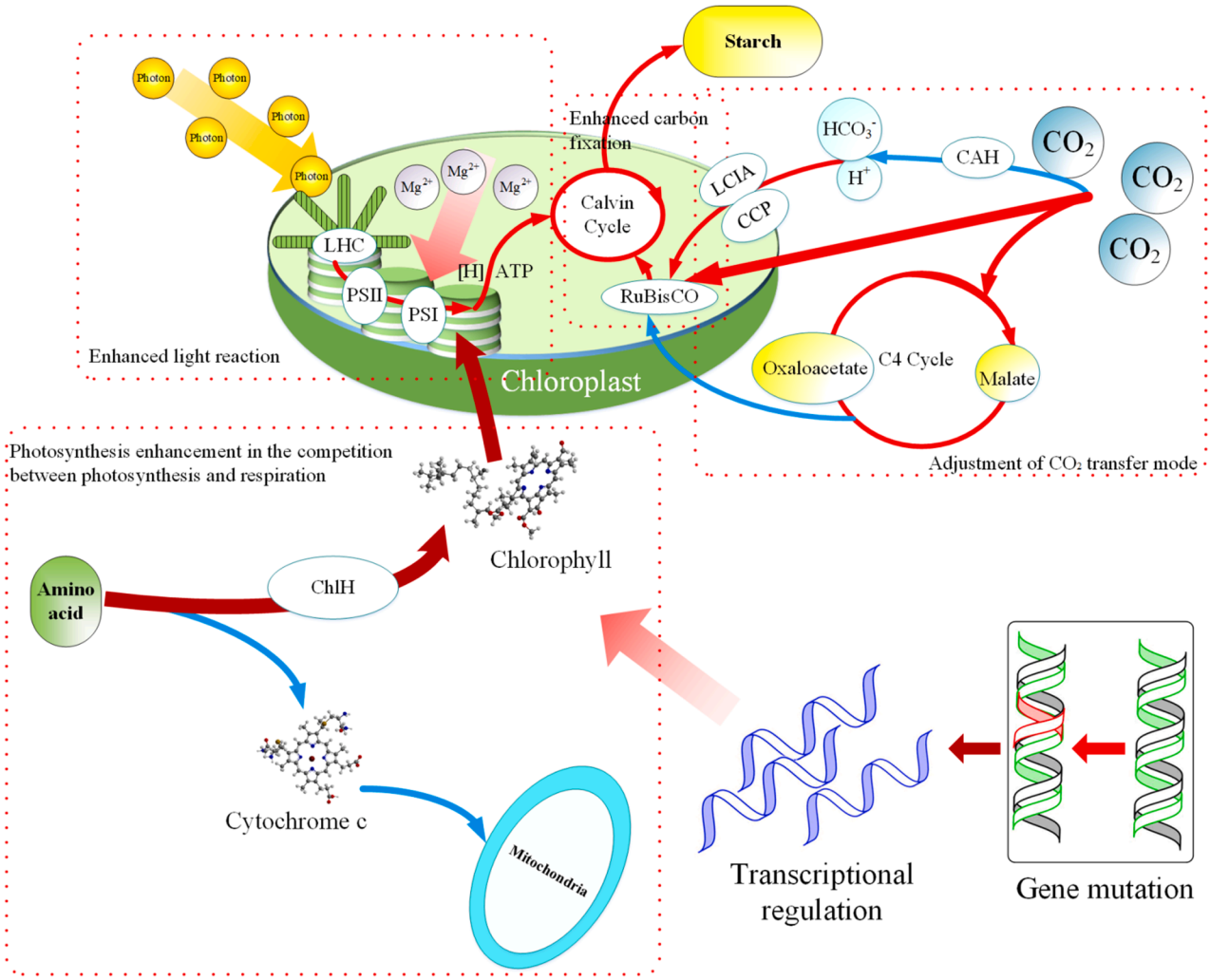

Fig. 9. A self-adaptive microalgae growth system of *N. oceanica* with gene mutation cored on cellular light response produced by CO_2 gradient domestication on 15% CO_2 adaption. Notes: Red arrow represents enhancement and blue arrow represents inhibition.

mechanism, which is centered on mutations of genes related to light response, especially within the pigment synthesis process, promotes the chlorophyll synthesis pathway and gave it an advantage over cytochrome *C* synthesis. Accordingly, the system regulated other physiological functions by promoting photosynthesis and inhibiting respiration. This means that the distribution of substances, energy and coenzymes in cell will be concentrated to the photosynthesis pathway. In response to these changes, the primary pathway for energy supply (ATP synthesis), which maintains normal intracellular physiological activity, must move from oxidative phosphorylation to photophosphorylation and substrate-level phosphorylation. Correspondingly, the transport of cation ion and sugar metabolism were also promoted because of their close relationship with chloroplast formation and carbon metabolism (glycolysis and synthesis of secondary metabolites). The former enhanced the photosynthetic linear electron transfer and cyclic electron transfer, which subsequently enhanced the corresponding ATP synthesis ability and improved the photoreaction efficiency, while the latter significantly enhanced substrate-level phosphorylation. Thus, in this new system of preferential photosynthesis, carbon fixation and energy supply are unified.

The enzymes involved in CCM mechanisms have shown their significance in this system. In other words, CCM mechanisms are not completely useless in high-carbon environments. High concentrations of CO_2 force CO_2 to dissolve and ionize both inside and outside the cell, which means there will be plenty of HCO_3^- in the cell (even if destruction of carbonic anhydrase by genetic engineering slows the reaction rate) until it is fixed by the Calvin Cycle. Therefore, within this self-adaptive system, in addition to the weakened conversion of CO_2 to HCO_3^-, active transporter of HCO_3^- to the chloroplast is unprecedently strengthened, and enabling HCO_3^- to be concentrated around the RuBisCO enzyme at a faster rate. The C4 pathway is another HCO_3^- concentration mechanism with a series complex steps to convert HCO_3^- to multiple carbon-containing compounds, and finally to CO_2 for Calvin Cycle. This pathway was universally strengthened but the rate at which the whole cycle is completed slows down. This means that the capacity of the C4 cycle is increased and more CO_2 will be stored as intermediates (such as malate and oxaloacetate) to relieve the high carbon pressure.

In this situation, high light reactions and the resulting carbohydrate synthesis may have accelerated intracellular metabolism and material accumulation, leading to faster division of single-celled *N. oceanica* CCMP1779. Therefore, another set of common genetic mutations occurred in the functions closely related to cell formation, including genetic material synthesis, transcription and translation. In contrast, enhanced CO_2 fixation enabled the cell to have a more stable internal environment (more balanced intracellular pH) and the possibility of cell destruction was reduced; thus, the proteolysis function degraded to a certain extent. These changes were immobilized as stable traits via genetic mutation and natural selection under environmental stress, and their effects were successfully observed at the transcriptional level.

Hence, fully domesticated strains of *N. oceanica* CCMP1779 showed more effective linear electron transport and cyclic electron transport for photosynthesis. Moreover, the light protection mechanism became more flexible and easier to recover, either during domestication, or under the high carbon conditions. Accordingly, in the dark reaction for CO_2 fixation, inorganic carbon transport was improved, the C4 mechanism for CO_2 storage became more powerful and the Calvin Cycle was enhanced. One hypothesis is that the core of these changes was the improved light-response genes. To adapt to a highly efficient light-response, the cell construction, ion transport, carbon metabolism, light reaction and dark reaction of *N. oceanica* CCMP1779 were improved during the process of domestication, so as to adapt to the high CO_2 environment. The principle of this self-adaptive mechanism will be useful when improving the CO_2 tolerance of microalgae.

5. Conclusion

This study performed a gradual gradient acclimation of CO_2 for *Nannochloropsis oceanica* CCMP1779 and subsequently carried out a comprehensive combined analysis of the genome, transcriptome, photosynthetic fluorescence, RT-qPCR and growth test under a high CO_2 environment to detect the effect and influencing mechanism of CO_2 gradient acclimation on microalgae. This study shows a potential mechanism for multi-targeted genetic mutations and natural selection to improve microalgal adaptation to high levels of CO_2, created spontaneously by the cells. This mechanism was based on improving the light response and favoring photosynthesis in the competition between photosynthesis and respiration, thereby comprehensively establishing a microalgal strain with new characteristics, including strong cell synthesis ability, photosynthetic electron transfer ability, carbon fixation and metabolism. As a result, this research revealed that functional selective multi-target gene mutation in microalgae is caused by the CO_2 gradient domestication process, resulting in improved photosynthesis, carbon fixation and cell synthesis.

This research demonstrated that CO_2 gradient domestication would lead to stable gene mutations of microalgae. As a simple and low-cost method, CO_2 gradient domestication was ideal to be applied in industry to the cultivation of high-CO_2 tolerant strains of various microalgae species. Therefore, this conclusion may help it be widely promoted to industrial applications, and help improve the industrial carbon fixation ability of microalgae.

Declaration of Competing Interest

The authors declare that they have no known competing financial interests or personal relationships that could have appeared to influence the work reported in this paper.

Acknowledgements

This study was supported by the National Key Research and Development Program-China (2017YFE0122800), and the Zhejiang Provincial Key Research and Development Program-China (2020C04006). We thank Yasuo Yoshikuni at the DOE Joint Genome Institute and Krishna Niyogi at the University of California Berkeley for their permission to use the genome of *N. oceanica* CCMP1779 (https://mycocosm.jgi.doe.gov/Nanoce1779_2/Nanoce1779_2.info.html) as the reference genome in this study.

Appendix A. Supplementary data

Supplementary data to this article can be found online at https://doi.org/10.1016/j.cej.2021.131968.

References

[1] A. Aslam, S.R. Thomas-Hall, T.A. Mughal, P.M. Schenk, Selection and adaptation of microalgae to growth in 100% unfiltered coal-fired flue gas, Bioresource Technol. 233 (2017) 271–283.

[2] A. Blanck, D. Oesterhelt, E. Ferrando, E.S. Schegk, F. Lottspeich, PRIMARY STRUCTURE OF SENSORY RHODOPSIN-I, A PROKARYOTIC PHOTORECEPTOR. EMBO J. 8 (1989) 3963–3971.

[3] A. Vieler, G.X. Wu, C.H. Tsai, B. Bullard, A.J. Cornish, C. Harvey, I.B. Reca, C. Thornburg, R. Achawanantakun, C.J. Buehl, M.S. Campbell, D. Cavalier, K. L. Childs, T.J. Clark, R. Deshpande, E. Erickson, A.A. Ferguson, W. Handee, Q. Kong, X.B. Li, B.S. Liu, S. Lundback, C. Peng, R.L. Roston, J.P. Sanjaya, A. Simpson, J. TerBush, S. Warakanont, E.M. Zauner, E.L. Farre, N. Hegg, M. H. Jiang, Y. Kuo, K.K. Lu, J. Niyogi, K.W. Ohlrogge, Y. Osteryoung, B.B. Shachar-Hill, Y.N. Sears, H. Sun, M. Takahashi, S.H.S. Yandell, C. Benning, Genome, Functional Gene Annotation, and Nuclear Transformation of the Heterokont Oleaginous Alga Nannochloropsis oceanica CCMP1779, PLoS Genet. 8 (2012) 1–25.

[4] A.G. Maqueo Chew, D.A. Bryant, Chlorophyll biosynthesis in bacteria: The origins of structural and functional diversity, Annu. Rev. Microbiol. 61 (2007) 113–129.

[5] A.M. Burger, A.K. Seth, The ubiquitin-mediated protein degradation pathway in cancer: therapeutic implications, Eur. J. Cancer 40 (2004) 2217–2229.
[6] D.D. Barker, C. Wang, J. Moore, L.K. Dickinson, R. Lehmann, Pumilio is essential for function but not for distribution of the Drosophila abdominal determinant Nanos, Gene. Dev. 6 (12a) (1992) 2312–2326.
[7] B.o. Yang, J. Liu, X. Ma, B. Guo, B. Liu, T. Wu, Y. Jiang, F. Chen, Genetic engineering of the Calvin cycle toward enhanced photosynthetic CO2 fixation in microalgae, Biotechnol. Biofuels 10 (1) (2017).
[8] B.L. Taylor, I.B. Zhulin, PAS domains: Internal sensors of oxygen, redox potential, and light, Microbiol. Mol. Biol. R. 63 (1999) 479.
[9] C.F. Chakarova, M.M. Hims, H. Bolz, L. Abu-Safieh, R.J. Patel, M.G. Papaioannou, C.F. Inglehearn, T.J. Keen, C. Willis, A.T. Moore, T. Rosenberg, A.R. Webster, A. C. Bird, A. Gal, D. Hunt, E.N. Vithana, S.S. Bhattacharya, Mutations in HPRP3, a third member of pre-mRNA splicing factor genes, implicated in autosomal dominant retinitis pigmentosa, Hum. Mol. Genet. 11 (2002) 87–92.
[10] C.W. Gee, K.K. Niyogi, The carbonic anhydrase CAH1 is an essential component of the carbon-concentrating mechanism in Nannochloropsis oceanica, P. Natl. Acad. Sci. Usa. 114 (2017) 4537–4542.
[11] D. Cheng, X. Li, Y. Yuan, C. Yang, T. Tang, Q. Zhao, Y. Sun, Adaptive evolution and carbon dioxide fixation of Chlorella sp. in simulated flue gas, Sci. Total Environ. 650 (2019) 2931–2938.
[12] D. Duanmu, A.R. Miller, K.M. Horken, D.P. Weeks, M.H. Spalding, Knockdown of limiting-CO2-induced gene HLA3 decreases HCO3- transport and photosynthetic Ci affinity in Chlamydomonas reinhardtii, P. Natl. Acad. Sci. Usa. 106 (2009) 5990–5995.
[13] D. Li, L. Wang, Q. Zhao, W. Wei, Y. Sun, Improving high carbon dioxide tolerance and carbon dioxide fixation capability of Chlorella sp by adaptive laboratory evolution, Bioresource Technol. 185 (2015) 269–275.
[14] D. Liu, Q. Ma, I. Valiela, D.M. Anderson, J.K. Keesing, K. Gao, Y.u. Zhen, X. Sun, Y. Wang, Role of C-4 carbon fixation in Ulva prolifera, the macroalga responsible for the world's largest green tides, COMMUNICATIONS BIOLOGY 3 (1) (2020).
[15] D. Oesterhelt, J. Tittor, 2 PUMPS, ONE PRINCIPLE - LIGHT-DRIVEN ION-TRANSPORT IN HALOBACTERIA, Trends Biochem. Sci. 14 (1989) 57–61.
[16] D. Tian, Q. Wang, P. Zhang, H. Araki, S. Yang, M. Kreitman, T. Nagylaki, R. Hudson, J. Bergelson, J. Chen, Single-nucleotide mutation rate increases close to insertions/deletions in eukaryotes, Nature 455 (2008) 105–170.
[17] D.F. Mello, R. Trevisan, N. Rivera, N.K. Geitner, R.T. Di Giulio, M.R. Wiesner, H. Hsu-Kim, J.N. Meyer, Caveats to the use of MTT, neutral red, Hoechst and Resazurin to measure silver nanoparticle cytotoxicity, Chem.-Biol. Interact. 315 (2020) 108868.
[18] D.W. Bollivar, Recent advances in chlorophyll biosynthesis, Photosynth. Res. 90 (2) (2007) 173–194.
[19] E. Bautista-Chamizo, A.R. Borrero-Santiago, M.R. De Orte, A. DelValls, I. Riba, Effects of CO2 enrichment on two microalgae species: A toxicity approach using consecutive generations, Chemosphere 213 (2018) 84–91.
[20] F. Li, Z. Yang, R. Zeng, G. Yang, X. Chang, J. Yan, Y. Hou, Microalgae Capture of CO2 from Actual Flue Gas Discharged from a Combustion Chamber, Ind. Eng. Chem. Res. 50 (2011) 6496–6502.
[21] F. Qi, D. Wu, R. Mu, S. Zhang, and X. Xu, Characterization of a Microalgal UV Mutant for CO2 Biofixation and Biomass Production. Biomed Res. Int. (2018).
[22] G. Huang, F. Chen, Y. Kuang, H. He, A.n. Qin, Current Techniques of Growing Algae Using Flue Gas from Exhaust Gas Industry: a Review, Appl. Biochem. Biotech. 178 (6) (2016) 1220–1238.
[23] G. Yu, L. Wang, Y. Han, Q. He, clusterProfiler: an R Package for Comparing Biological Themes Among Gene Clusters, OMICS 16 (2012) 284–287.
[24] G.H. Lorimer, M.R. Badger, T.J. Andrews, ACTIVATION OF RIBULOSE-1,5-BISPHOSPHATE CARBOXYLASE BY CARBON-DIOXIDE AND MAGNESIUM-IONS - EQUILIBRIA, KINETICS, A SUGGESTED MECHANISM, AND PHYSIOLOGICAL IMPLICATIONS. Biochemistry-US 15 (1976) 529–536.
[25] G.M. Lima, P.C.N. Teixeira, C.M.L.L. Teixeira, D. Filocomo, C.L.S. Lage, Influence of spectral light quality on the pigment concentrations and biomass productivity of Arthrospira platensis, Algal Res. 31 (2018) 157–166.
[26] H.M. Singh, R. Kothari, R. Gupta, V.V. Tyagi, Bio-fixation of flue gas from thermal power plants with algal biomass: Overview and research perspectives, J. Environ. Manage. 245 (2019) 519–539.
[27] I. Rumak, K. Gieczewska, B. Kierdaszuk, W.I. Gruszecki, A. Mostowska, R. Mazur, M. Garstka, 3-D modelling of chloroplast structure under (Mg2+) magnesium ion treatment. Relationship between thylakoid membrane arrangement and stacking, Bba.-Bioenergetics 1797 (2010) 1736–1748.
[28] J. Cheng, H. Lu, X. He, W. Yang, J. Zhou, K. Cen, Mutation of Spirulina sp by nuclear irradiation to improve growth rate under 15% carbon dioxide in flue gas, Bioresource Technol. 238 (2017) 650–656.
[29] J. Cheng, H.X. Lu, Y. Huang, K. Li, R. Huang, J.H. Zhou, K.F. Cen, Enhancing growth rate and lipid yield of Chlorella with nuclear irradiation under high salt and CO2 stress, Bioresource Technol. 203 (2016) 220–227.
[30] J. Cheng, K. Li, Z. Yang, H. Lu, J. Zhou, K. Cen, Gradient domestication of Haematococcus pluvialis mutant with 15% CO2 to promote biomass growth and astaxanthin yield, Bioresource Technol. 216 (2016) 340–344.
[31] J. Cheng, Y. Huang, J. Feng, J. Sun, J. Zhou, K. Cen, Mutate Chlorella sp by nuclear irradiation to fix high concentrations of CO2, Bioresource Technol. 136 (2013) 496–501.
[32] J. Cheng, Y. Zhu, Z.e. Zhang, W. Yang, Modification and improvement of microalgae strains for strengthening CO2 fixation from coal-fired flue gas in power plants, Bioresource Technol. 291 (2019) 121850.
[33] J. Cheng, Z. Wang, H. Lu, W. Yang, Z. Fan, Hydrogen Sulfide Improves Lipid Accumulation in Nannochloropsis oceanica through Metabolic Regulation of Carbon Allocation and Energy Supply, ACS Sustain. Chem. Eng. 8 (2020) 2481–2489.
[34] J. Li, X. Tang, K. Pan, B. Zhu, Y. Li, X. Ma, Y. Zhao, The regulating mechanisms of CO2 fixation and carbon allocations of two Chlorella sp. strains in response to high CO2 levels, Chemosphere 247 (2020), 125814.
[35] J. Roberto Ramos-Ibarra, R. Snell-Castro, J. Alejandro Neria-Casillas, F.J. Choix, Biotechnological potential of Chlorella sp. and Scenedesmus sp. microalgae to endure high CO2 and methane concentrations from biogas, Bioproc. Biosyst. Eng. 42 (2019) 1603–1610.
[36] J. Tao, L. Feng, H.J. Guo, Y.Y. Li, L. Wang, The O-antigen gene cluster of Shigella boydii O11 and functional identification of its wzy gene, FEMS Microbiol. Lett. 234 (2004) 125–132.
[37] J. Vikramathithan, K. Hwangbo, J.-M. Lim, K.-M. Lim, D.Y. Kang, Y.-I. Park, W.-J. Jeong, Overexpression of Chlamydomonas reinhardtii LCIA (CrLCIA) gene increases growth of Nannochloropsis salina CCMP1776, Algal Res. 46 (2020) 101807.
[38] J. Zhang, W. Tsai, C. Hsu, C. Peng, Biodiesel production from Nannochloropsis oculata cultured at stressful carbon dioxide concentration and light illumination, BIOFUELS-UK (2020).
[39] J.D. Hollister, J. Ross-Ibarra, B.S. Gaut, Indel-Associated Mutation Rate Varies with Mating System in Flowering Plants, Mol. Biol. Evol. 27 (2010) 409–416.
[40] J.M. Frustaci, M.R. Obrian, CHARACTERIZATION OF A BRADYRHIZOBIUM-JAPONICUM FERROCHELATASE MUTANT AND ISOLATION OF THE HEMH GENE, J. Bacteriol. 174 (1992) 4223–4229.
[41] J.R. Casey, S. Grinstein, J. Orlowski, Sensors and regulators of intracellular pH, Nat. Rev. Mol. Cell Bio. 11 (1) (2010) 50–61.
[42] J.V. Moroney, Y. Ma, W.D. Frey, K.A. Fusilier, T.T. Pham, T.A. Simms, R. J. DiMario, J. Yang, B. Mukherjee, The carbonic anhydrase isoforms of Chlamydomonas reinhardtii: intracellular location, expression, and physiological roles, Photosynth. Res. 109 (2011) 133–149.
[43] K. Maxwell, G.N. Johnson, Chlorophyll fluorescence - a practical guide, J. Exp. Bot. 51 (2000) 659–668.
[44] K. Miura, T. Yamano, S. Yoshioka, T. Kohinata, Y. Inoue, F. Taniguchi, E. Asamizu, Y. Nakamura, S. Tabata, K.T. Yamato, K. Ohyama, H. Fukuzawa, Expression profiling-based identification of CO2-responsive genes regulated by CCM1 controlling a carbon-concentrating mechanism in Chlamydomonas reinhardtii, Plant Physiol. 135 (2004) 1595–1607.
[45] K. Rohacek, M. Bartak, Technique of the modulated chlorophyll fluorescence: basic concepts, useful parameters, and some applications, Photosynthetica 37 (1999) 339–363.
[46] L. Dall'Osto, M. Bressan, R. Bassi, Biogenesis of light harvesting proteins, Bba.-Bioenergetics 1847 (2015) 861–871.
[47] L. Wei, C. Shen, M. El Hajjami, W. You, Q. Wang, P. Zhang, Y. Ji, H. Hu, Q. Hu, A. Poetsch, J. Xu, Knockdown of carbonate anhydrase elevates Nannochloropsis productivity at high CO2 level, Metab. Eng. 54 (2019) 96–108.
[48] L. Wei, Y. Xin, Q. Wang, J. Yang, H. Hu, J. Xu, RNAi-based targeted gene knockdown in the model oleaginous microalgae Nannochloropsis oceanica, Plant J. 89 (2017) 1236–1250.
[49] M. Jeanneau, D. Gerentes, X. Foueillassar, M. Zivy, J. Vidal, A. Toppan, P. Perez, Improvement of drought tolerance in maize: towards the functional validation of the Zm-Asr1 gene and increase of water use efficiency by over-expressing C4-PEPC, Biochimie 84 (2002) 1127–1135.
[50] M. Li, J. Wang, Y. Geng, Y. Li, Q. Wang, Q. Liang, Q. Qi, A strategy of gene overexpression based on tandem repetitive promoters in Escherichia coli, Microb. Cell Fact. 11 (1) (2012) 19.
[51] M. Pertea, D. Kim, G.M. Pertea, J.T. Leek, S.L. Salzberg, Transcript-level expression analysis of RNA-seq experiments with HISAT, StringTie and Ballgown. Nat. Protoc. 11 (9) (2016) 1650–1667.
[52] M. Wyganowska-Swiatkowska, M. Tarnowski, D. Murtagh, E. Skrzypczak-Jankun, J. Jankun, Proteolysis is the most fundamental property of malignancy and its inhibition may be used therapeutically (Review), Int. J. Mol. Med. 43 (2019) 15–25.
[53] M.G. de Morais, J.A. Vieira Costa, Isolation and selection of microalgae from coal fired thermoelectric power plant for biofixation of carbon dioxide, Energ. Convers. Manage. 48 (2007) 2169–2173.
[54] M.H. Spalding, M. Jeffrey, MEMBRANE-ASSOCIATED POLYPEPTIDES INDUCED IN CHLAMYDOMONAS BY LIMITING CO2 CONCENTRATIONS, Plant Physiol. 89 (1989) 133–137.
[55] M.S. Jones, O. Jones, STRUCTURAL ORGANIZATION OF HAEM SYNTHESIS IN RAT LIVER MITOCHONDRIA, Biochem. J. 113 (1969) 507.
[56] N. Yan, Structural Biology of the Major Facilitator Superfamily Transporters. in: K. A. Dill, (Ed.), Annual Review of Biophysics, (2015) 257-283.
[57] P. Tcvetkov, A. Cherepovitsyn, S. Fedoseev, The Changing Role of CO2 in the Transition to a Circular Economy: Review of Carbon Sequestration Projects, Sustainability-Basel 11 (20) (2019) 5834.
[58] P. Wang, B. Grimm, Organization of chlorophyll biosynthesis and insertion of chlorophyll into the chlorophyll-binding proteins in chloroplasts, Photosynth. Res. 126 (2015) 189–202.
[59] P. Wang, J. Heitman, The cyclophilins. GENOME BIOLOGY 6 (2005).
[60] P.A. Burrows, L.A. Sazanov, Z. Svab, P. Maliga, P.J. Nixon, Identification of a functional respiratory complex in chloroplasts through analysis of tobacco mutants containing disrupted plastid ndh genes, EMBO J. 17 (1998) 868–876.
[61] R. Sharon-Gojman, S. Leu, A. Zarka, Antenna size reduction and altered division cycles in self-cloned, marker-free genetically modified strains of Haematococcus pluvialis, Algal Res. 28 (2017) 172–183.

[62] R.A. Cairns, I.S. Harris, T.W. Mak, Regulation of cancer cell metabolism, Nat. Rev. Cancer 11 (2) (2011) 85–95.
[63] R.A.S. Lestari, E.P. Nurlaili, and P. Kusumo, The Effect of Carbon Dioxide Concentration and the Dimension of Photobioreactor on the Growth of Microalgae Nannochloropsis sp. in: M. Anwar, F. Adriyanto, S. Pramono, H. Maghfiroh, C. Apribowo, S. Ibrahim, M.E. Sulistyo, and M.H. Ibrahim, (Eds.), AIP Conference Proceedings, (2019).
[64] R.J. Porra, W.A. Thompson, P.E. Kriedemann, DETERMINATION OF ACCURATE EXTINCTION COEFFICIENTS AND SIMULTANEOUS-EQUATIONS FOR ASSAYING CHLOROPHYLL-A AND CHLOROPHYLL-B EXTRACTED WITH 4 DIFFERENT SOLVENTS - VERIFICATION OF THE CONCENTRATION OF CHLOROPHYLL STANDARDS BY ATOMIC-ABSORPTION SPECTROSCOPY, BIOCHIMICA ET BIOPHYSICA ACTA 975 (1989) 384–394.
[65] R.P. Ross, A. Claiborne, MOLECULAR-CLONING AND ANALYSIS OF THE GENE ENCODING THE NADH OXIDASE FROM STREPTOCOCCUS-FAECALIS 10C1 - COMPARISON WITH NADH PEROXIDASE AND THE FLAVOPROTEIN DISULFIDE REDUCTASES, J. Mol. Biol. 227 (1992) 658–671.
[66] S. Chiu, C. Kao, C. Chen, T. Kuan, S. Ong, C. Lin, Reduction of CO2 by a high-density culture of Chlorella sp in a semicontinuous photobioreactor, Bioresource Technol. 99 (2008) 3389–3396.
[67] S. Chiu, C. Kao, M. Tsai, S. Ong, C. Chen, C. Lin, Lipid accumulation and CO2 utilization of Nannochloropsis oculata in response to CO2 aeration, Bioresource Technol. 100 (2009) 833–838.
[68] S. Paul, A. Banerjee, and A. Roychoudhury, Role of Polyamines in Mediating Antioxidant Defense and Epigenetic Regulation in Plants Exposed to Heavy Metal Toxicity. in: H. M., N. K., and F. M., (Eds.), Plants Under Metal and Metalloid Stress, Springer, Singapore, (2018).
[69] S. Takahashi, T. Kuzuyama, H. Watanabe, H. Seto, A 1-deoxy-D-xylulose 5-phosphate reductoisomerase catalyzing the formation of 2-C-methyl-D-elythritol 4-phosphate in an alternative nonmevalonate pathway for terpenoid biosynthesis, P. Natl. Acad. Sci. Usa. 95 (1998) 9879–9884.
[70] S. Wang, L. Zheng, X. Han, B. Yang, J. Li, C. Sun, Lipid accumulation and CO2 utilization of two marine oil-rich microalgal strains in response to CO2 aeration, Acta Oceanol. Sin. 37 (2018) 119–126.
[71] S. Yalcin, A.E.S. Konukman, A. Midilli, Present and future of flue gas emission reduction technologies related to fossil power generation, Greenh, Gases, 2020.
[72] S.S. Mande, D. Parsonage, A. Claiborne, W. Hol, CRYSTALLOGRAPHIC ANALYSES OF NADH PEROXIDASE CYS42ALA AND CYS42SER MUTANTS - ACTIVE-SITE STRUCTURES, MECHANISTIC IMPLICATIONS, AND AN UNUSUAL ENVIRONMENT OF ARG-303, Biochemistry-US 34 (1995) 6985–6992.
[73] S.S. Mande, S. Sarfaty, M.D. Allen, R.N. Perham, W. Hol, Protein-protein interactions in the pyruvate dehydrogenase multienzyme complex: Dihydrolipoamide dehydrogenase complexed with the binding domain of dihydrolipoamide acetyltransferase, Structure 4 (1996) 277–286.
[74] T. Senda, T. Yamada, N. Sakurai, M. Kubota, T. Nishizaki, E. Masai, M. Fukuda, Y. Mitsui, Crystal structure of NADH-dependent ferredoxin reductase component in biphenyl dioxygenase, J. Mol. Biol. 304 (2000) 397–410.
[75] T.C. Pedersen, R.D. Gardner, R. Gerlach, B.M. Peyton, Assessment of Nannochloropsis gaditana growth and lipid accumulation with increased inorganic carbon delivery, J. Appl. Phycol. 30 (2018) 2155–2166.
[76] V. Doubnerova, H. Ryslava, What can enzymes of C-4 photosynthesis do for C-3 plants under stress? Plant Sci. 180 (2011) 575–583.
[77] V.A. Portnoy, D. Bezdan, K. Zengler, Adaptive laboratory evolution - harnessing the power of biology for metabolic engineering, Curr. Opin. Biotech. 22 (2011) 590–594.
[78] Y. Chen, C. Xu, S. Vaidyanathan, Influence of gas management on biochemical conversion of CO2 by microalgae for biofuel production, Appl. Energ. 261 (2020) 114420.
[79] Y. Deng, J.Y. Ye, H.L. Mi, Effects of low CO2 on NAD(P)H dehydrogenase, a mediator of cyclic electron transport around photosystem I in the cyanobacterium Synechocystis PCC6803, Plant Cell Physiol. 44 (2003) 534–540.
[80] Y. Taniguchi, H. Ohkawa, C. Masumoto, T. Fukuda, T. Tamai, K. Lee, S. Sudoh, H. Tsuchida, H. Sasaki, H. Fukayama, M. Miyao, Overproduction of C(4) photosynthetic enzymes in transgenic rice plants: an approach to introduce the C (4)-like photosynthetic pathway into rice, J. Exp. Bot. 59 (2008) 1799–1809.
[81] Y. Wang, M.H. Spalding, Acclimation to Very Low CO2: Contribution of Limiting CO2 Inducible Proteins, LCIB and LCIA, to Inorganic Carbon Uptake in Chlamydomonas reinhardtii(1[OPEN]), Plant Physiol. 166 (2014) 2040–2050.
[82] Y. Zhu, J. Cheng, X. Xu, H. Lu, Y. Wang, X. Li, W. Yang, Using polyethylene glycol to promote Nannochloropsis oceanica growth with 15 vol% CO2, Sci. Total Environ. 720 (2020).
[83] Z. Liu, F. Zhang, F. Chen, High throughput screening of CO2-tolerating microalgae using GasPak bags, Aquatic biosystems 9 (2013) 23.
[84] Z. Liu, K. Wang, Y. Chen, T. Tan, J. Nielsen, Third-generation biorefineries as the means to produce fuels and chemicals from CO2, NATURE CATALYSIS 3 (2020) 274–288.